Economic Geology
Vol. 98, 2003, pp. 1225–1241

Alligator Ridge District, East-Central Nevada: Carlin-Type Gold Mineralization at Shallow Depths

CONSTANCE J. NUTT† AND ALBERT H. HOFSTRA

U. S. Geological Survey, Mail Stop 905, P. O. Box 25046, Denver, Colorado 80225

Abstract

Carlin-type deposits in the Alligator Ridge mining district are present sporadically for 40 km along the north-striking Mooney Basin fault system but are restricted to a 250-m interval of Devonian to Mississippian strata. Their age is bracketed between silicified ca. 45 Ma sedimentary rocks and unaltered 36.5 to 34 Ma volcanic rocks. The silicification is linked to the deposits by its continuity with ore-grade silicification in Devonian-Mississippian strata and by its similar $\delta^{18}O$ values (~17‰) and trace element signature (As, Sb, Tl, Hg). Eocene reconstruction indicates that the deposits formed at depths of ≤300 to 800 m. In comparison to most Carlin-type gold deposits, they have lower Au/Ag, Au grades, and contained Au, more abundant jasperoid, and textural evidence for deposition of an amorphous silica precursor in jasperoid. These differences most likely result from their shallow depth of formation.

The peak fluid temperature (~230°C) and large $\delta^{18}O_{H2O}$ value shift from the meteroric water line (~20‰) suggest that ore fluids were derived from depths of 8 km or more. A magnetotelluric survey indicates that the Mooney Basin fault system penetrates to mid-crustal depths. Deep circulation of meteoric water along the Mooney Basin fault system may have been in response to initial uplift of the East Humboldt-Ruby Mountains metamorphic core complex; convection also may have been promoted by increased heat flow associated with large magnitude extension in the core complex and regional magmatism. Ore fluids ascended along the fault system until they encountered impermeable Devonian and Mississippian shales, at which point they moved laterally through permeable strata in the Devonian Guilmette Formation, Devonian-Mississippian Pilot Shale, Mississippian Joana Limestone, and Mississippian Chainman Shale toward erosional windows where they ascended into Eocene fluvial conglomerates and lake sediments. Most gold precipitated by sulfidation of host-rock Fe and mixing with local ground water in zones of lateral fluid flow in reactive strata, such as the Lower Devonian-Mississippian Pilot Shale.

Introduction

THE ALLIGATOR RIDGE mining district is in east-central Nevada, about 115 km south-southeast of Elko and about 100 km northwest of Ely (Figs. 1, 2a). The gold district is on the southern extension of the northwest-striking, 60-km-long Carlin trend that is estimated to contain >100 Moz of Au in more than 40 separate deposits with average Au grades of 1 to 25 g/t and Au/Ag between 3 and 20 (Hofstra and Cline, 2000; Teal and Wright, 2000). These Carlin-type deposits formed at depths of 0 to 5 km (Hofstra and Cline, 2000). The major ore-forming event in the Carlin trend is interpreted to have been Eocene by Emsbo et al. (1996), Henry and Boden (1998), Hofstra et al. (1999), and Ressel et al. (2000). Alligator Ridge belongs to a belt of small-tonnage, low-grade gold deposits, including the Illipah deposit (Figs. 1, 2a), that are hosted by Devonian and Mississippian sedimentary rocks and are considered a subtype of Carlin-type deposits (Maher, 1997). The Alligator Ridge deposits are the largest of this type (Maher, 1997). The study area is east and southeast of the Bald Mountain mining district (Fig. 2b), which contains gold deposits interpreted to be related to a Jurassic intrusion (Hitchborn et al., 1996; Nutt et al., 2000). Previously published work in the area includes a regional geologic map (Rigby, 1960), the White Pine County geologic map (Hose and Blake, 1976), and studies of the Alligator Ridge district gold deposits, of which the most comprehensive is on the Vantage deposits by Ilchik (1990a). Nutt et al. (2000) describe the Bald Mountain and Alligator Ridge districts. This paper's contributions to the understanding of the district are based on new mapping at a 1:24,000 scale by Nutt (2000) and C.J. Nutt and K.S. Hart (unpub. data, 2002) and include new descriptions of Eocene rocks, evidence for the depth and age

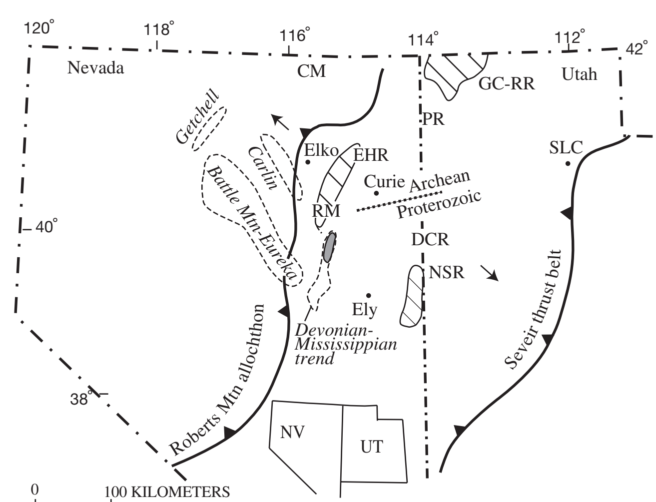

FIG. 1. The Alligator Ridge district, shown in dark gray, in relation to nearby Au trends (short dashed outlines) and geologic features in northeastern Nevada and northwestern Utah. CM = general location of Copper Mountains, DCR = Deep Creek Range, EHR = East Humboldt Range, GC-RR = Grouse Creek-Raft River Mountains, NSR = Northern Snake Range, PR = Pilot Range, RM = Ruby Mountains, SLC = Salt Lake City. Core complexes shown by diagonal lines. Devonian-Mississippian Au trend from Maher (1997), approximate boundary between Archean and Proterozoic crust from Wooden et al. (1998). Arrows represent extension direction in the Eocene.

† Corresponding author: e-mail, cnutt@usgs.gov, ahofstra@usgs.gov

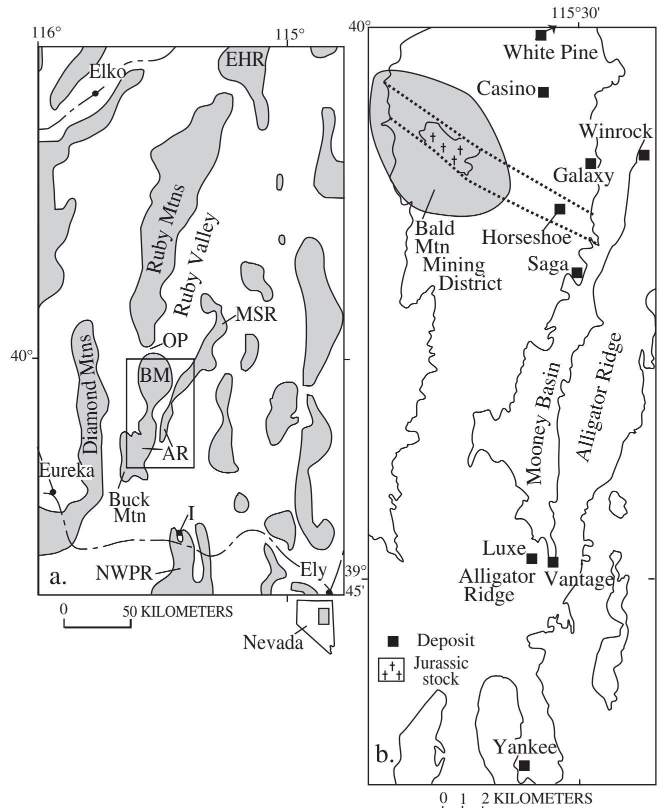

FIG. 2. Locality maps. a. Alligator Ridge area in eastern Nevada. AR = Alligator Ridge, BM = Bald Mountain, EHR = East Humboldt Range, I = Illipah, MSR = Maverick Springs Range, NWPR = northern White Pine Range, OP = Overland Pass. Rectangle is area of (b). b. Carlin-type deposits and geographic features in the Alligator Ridge area. Bida trend shown by dashed lines in Bald Mountain area

of mineralization and a crustal structural control, and the results of petrographic, SEM, electron microprobe, lithogeochemical, and stable isotope studies of jasperoid and carbonaceous ore in deposits other than Vantage. These data, combined with a synthesis and reinterpretation of previous work, allow us to constrain the age of mineralization and develop an improved model of the Eocene geologic setting, fluid-flow paths, and depth of formation of the deposits. An inferred shallow depth of formation explains some distinctive characteristics of the deposits and the abundance of jasperoid in the district.

Geologic Setting

The Alligator Ridge district is underlain by Late Proterozoic (?) and Paleozoic miogeoclinal carbonate and clastic rocks deposited on the North American continental margin following Proterozoic rifting. The district is in the foreland of the Devonian-Mississippian Antler orogenic belt where eugeoclinal rocks of the Roberts Mountains allochthon were emplaced from the west over miogeoclinal and slope-deposited rocks (Fig. 1). In the east is the hinterland of the Jurassic, Cretaceous, and early Tertiary Sevier orogenic belt of thin-skinned deformation that also moved rocks in an easterly direction. Following Mesozoic to early Tertiary contractional deformation, Tertiary extension affected the Great basin. The Alligator Ridge area is in a north- to northeast-trending regional corridor of large-magnitude extension and core complexes.

Stratigraphy

Rocks exposed in the Alligator Ridge district are Devonian through Permian miogeoclinal carbonate and clastic rocks, Tertiary sedimentary and volcanic rocks, and at and near the Horseshoe deposit, Jurassic intrusive rock (Fig. 3). Just west of the district, at Bald Mountain, Cambrian through Ordovician clastic and carbonate rocks and a 159 Ma quartz monzonite porphyry stock crop out (Mortensen et al., 2000; Fig. 3). In the district, ore is hosted mainly by Devonian and Mississippian rocks and, at Horseshoe, by Jurassic intrusive rock.

The gold deposits are predominantly in thin-bedded units, preferentially at and above contacts between thick-bedded to massive carbonate and overlying calcareous clastic units (Fig. 4). The primary host is the Devonian to Mississippian Pilot Shale, which consists of calcareous, dolomitic, and in places, carbonaceous, siltstone, shale, and thin-bedded limestone overlying thick-bedded limestone in the Devonian Guilmette Formation. Secondary hosts are the Mississippian Joana Limestone and overlying Mississippian Chainman Shale. The Joana Limestone is typically a thin-bedded crinoidal limestone and is silicified to jasperoid where gold bearing. The Chainman Shale, which hosts the Winrock deposit (Figs. 2b, 4), consists of shale, in part carbonaceous, and subordinate thin-bedded limestone, siltstone, and sandstone. Ore at the Horseshoe deposit is in both the Pilot Shale and a Jurassic porphyry dike; ore in the porphyry is restricted to where it intrudes the Pilot Shale. The Pilot Shale is partly age correlative with the Devonian to Mississippian Woodruff Formation, the Devonian Popovich Formation, and the informal Rodeo Creek unit, which are important host rocks in the Carlin trend; however, the Pilot Shale formed in a separate basin south and southeast of the Carlin trend (Maher, 1997; F.G. Poole, written commun., 2002).

Throughout the district, the contact between the Pilot Shale and Guilmette Formation is marked by a discontinuous, thickening (up to 35 m) and thinning jasperoid that primarily is in the upper Guilmette Formation but in places extends into the lower Pilot Shale (Ilchik, 1990a, and references therein). The jasperoid-forming event silicified Jurassic intrusive rocks along the Guilmette-Pilot contact and replaced folded Paleozoic rocks. The jasperoid is locally ore. The top of the Guilmette Formation has anomalous amounts of authigenic barite in isolated crystals and rosettes (Ilchik, 1990a; this study) and contains a few isolated occurrences of hydrothermal dolomite with conspicuous gray and white banding, also known as "zebra dolomite." Certain horizons in the overlying Pilot and Chainman Shales have anomalous concentrations of Ba, Hg, Se, Ni, Mo, Ag, and base metals (Placer Dome North America, Inc., unpubl. data, 2002). These features may be due to minor Late Devonian to Early Mississippian sedimentary exhalative hydrothermal activity similar to that described by Emsbo et al. (1999) in the Carlin trend.

Tertiary rocks, which are described in detail below, include lacustrine limestone, clastic rocks, volcaniclastic rocks, tuffs, and volcanic flows. The Tertiary volcanic rocks are exposed

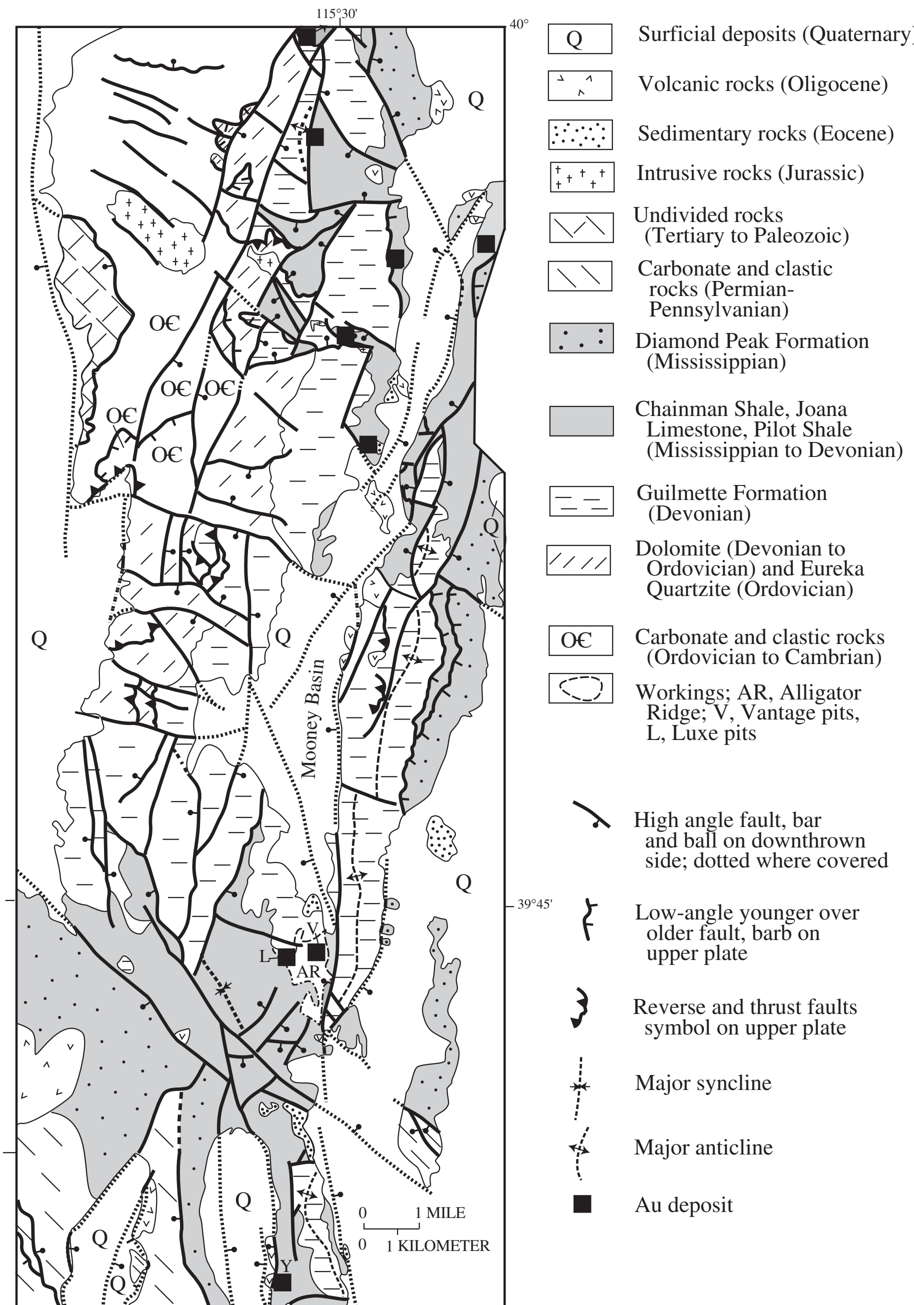

FIG. 3. Geologic map of the Alligator Ridge area. Simplified from Nutt (2000) and C.J. Nutt and K.S. Hart (unpub. data, 2002). AR = Alligator Ridge area, L = Luxe deposit, V = Vantage deposit, Y = Yankee deposit.

throughout the area, but the sedimentary rocks are restricted to the east side of the district. Unaltered Eocene to Oligocene volcanic rocks lie on silicified rocks associated with mineralization and are therefore interpreted to postdate mineralization. Although ca. 35 Ma, poorly to moderately consolidated tuff contains smectite, the lack of silicified tuff, sulfide minerals (or supergene limonite), or anomalous concentrations of trace elements suggests that the smectite formed by devitrification of volcanic glass, interaction with ground waters, and weathering.

Regional structure

The Alligator Ridge district is characterized by kilometer-long folds and faults. The folds are north to northeast trending and gentle, except at Alligator Ridge where the fold is overturned. Ore at the Yankee, Vantage, Luxe, and Casino deposits is on the limbs of folds.

Two major sets of faults are present throughout the district. North-northeast-striking faults are typically long, whereas northwest-striking faults are short and in places en echelon

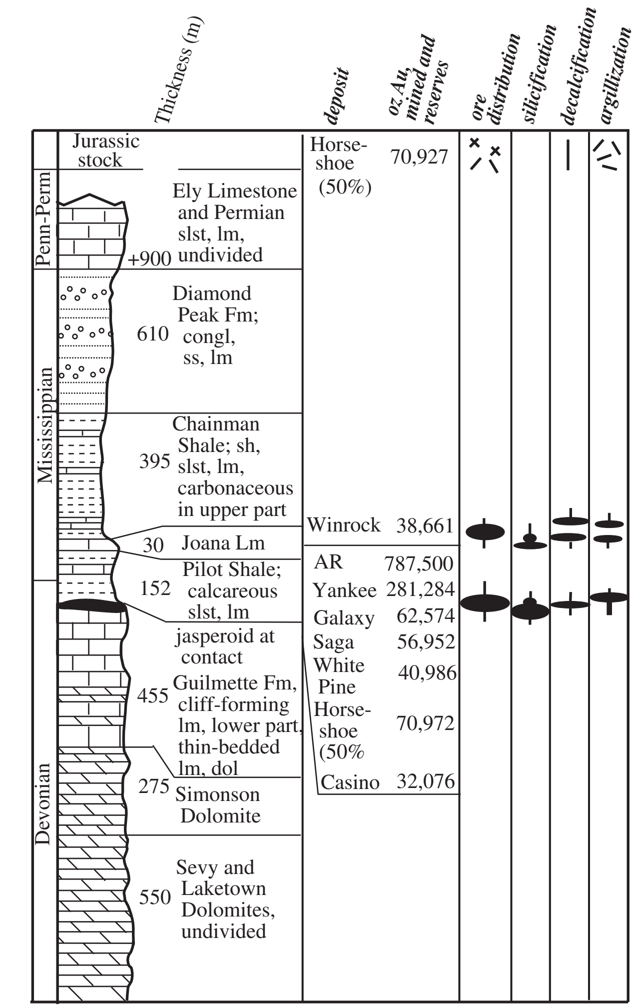

FIG. 4. Stratigraphic column of Paleozoic rocks in Alligator Ridge district; strata-bound jasperoid shown in black. "Deposits," "oz Au, mined and reserves," "ore distribution," "silicification," "decalcification" and "argillization" are shown in columns. Patterns in columns: dash = disseminated, vertical line = discordant, elliptical shape = strata bound, **x** = stockwork. Abbreviations: AR = Alligator Ridge, congl = conglomerate, dol = dolomite, Fm = Formation, lm = limestone, sh = shale, slst = siltstone, ss = sandstone.

(Fig. 3). The most important of the north-northeast-striking structures is a fault system along Mooney basin, which extends from tne Yankee deposit in the south to the north end of the district; gold deposits occur along or near this feature. Early reverse movement along this fault and north-trending folds are probably related to Sevier-age deformation. Based on a regional magnetotelluric survey from west of Eureka, Nevada, to east of Mooney basin, Rodriguez and Williams (2001) interpreted a north-striking crustal-scale fault system that is largely coincident with the Mooney basin. B.D. Rodriguez (written commun., 2002) interprets the fault system as extending at least the length of the district and probably north of the map area into Ruby Valley. The Bida trend (Fig. 2b) is the largest of the northwest-striking fault zones and controlled emplacement of the Jurassic Bald Mountain stock. The Horseshoe deposit is near the intersection of the Bida trend and the Mooney Basin fault system.

Regional Eocene tectonic and magmatic setting

In the Eocene, the eastern Great Basin was characterized by the change from Cretaceous and early Tertiary contraction (Sevier orogeny) to crustal extension, calc-alkaline magmatism, and formation of sedimentary basins. The change from contraction to extension may be related to the slowing of plate convergence between the Farallon and North American plates (Stock and Molnar, 1988) and/or slab rollback (Dickinson, 2001, 2002). The Eocene igneous rocks are part of a southward-migrating pattern of magmatism (Christiansen et al., 1992) that began in British Columbia about 55 Ma.

Eocene nonmarine sedimentary rocks underlie volcanic rocks at some localities in northeast Nevada. Typical sequences consist of a basal conglomerate overlain by volcaniclastic rocks, sandstone, shale, and lacustrine limestone (Brooks et al., 1995). The largest recognized basins include the Elko basin near Elko, Nevada (Solomon et al., 1979; Ketner and Alpha, 1992), the Bull Run basin northeast of Elko (Clark and Ehman, 1985), and the Sheep Pass Formation about 200 km south and east of Elko (Fouch et al., 1979, 1992). Most sedimentation in these basins occurred in the Eocene, but in some basins it started as early as latest Cretaceous and continued into the Oligocene. The presence of a 46.1 Ma tuff near the base of the Elko Formation indicates that some volcanism accompanied sedimentation (Haynes et al., 2002). The presence of ostracod lacustrine limestone suggests that Eocene sedimentation took place in shallow lakes or marshes.

Eocene extensional uplift was centered in the core complexes (see Fig. 1), which are known mostly for their Miocene uplift (Miller et al., 1999). Armstrong (1968) proposed little topographic relief on the early Tertiary paleosurface, but recent work suggests that domains locally were substantially extended. For example, McGrew and Snee (1994), who studied the East Humboldt Range-Ruby Mountains core complex near the northern end of the Alligator Ridge district, used $^{40}Ar/^{39}Ar$ ages of hornblende to suggest that rocks at high structural levels were uplifted in the early Tertiary (63–49 Ma). Expanding on this work, McGrew et al. (2000) proposed Late Cretaceous to early Tertiary tectonic denudation of at least 7 km in the east Humboldt Range and suggested a steepened geothermal gradient. Southeast of the Alligator Ridge district, Gans et al. (2001) showed evidence of rapid Eocene extension at 37.6 to 36.8 Ma in the Robinson mining district near Ely, Nevada. Other places where Eocene deformation is documented include the Copper Mountains (Rahl et al., 2002) and northern Snake Range (Lee, 1995) in Nevada and the Pilot Range (Miller et al., 1987), Grouse Creek-Raft River Mountains (Wells et al., 2000), and Deep Creek Range (Potter et al., 1995) in Utah and Nevada.

Eocene stratigraphy of Alligator Ridge

In the Alligator Ridge district, rhyolite flows and domes, quartz-biotite tuff, and intermediate composition flows are late Eocene to early Oligocene in age. They lie on Devonian to Permian rocks and, locally, on Tertiary sedimentary rocks. A rhyolite dike in the northeast Mooney basin yielded a zircon U-Pb age of 35.9 ± 0.1 Ma (Mortensen et al., 2000) and is similar in composition to a nearby rhyolite dome. Just east of the study area, $^{40}Ar/^{39}Ar$ age determinations on biotites from two rhyolite flows overlying Pennsylvanian and Permian rocks are 36.27 ± 0.11 Ma and 36.56 ± 0.10 Ma (R.J. Fleck, written commun., 1999). Sanidine from a basal reworked quartz-biotite lithic tuff near Alligator Ridge yielded a $^{40}Ar/^{39}Ar$ date of 34.99 ± 0.08 Ma (Nutt, 2000). In the northern White Pine Range to the south, the oldest documented Tertiary volcanic rock is 38.1 ± 0.2 Ma (Gans, 2000).

The most abundant Eocene sedimentary rocks are conglomerate, sandstone, shale, lacustrine limestone, and volcaniclastic rocks. The limestone is dated as latest early to early, middle Eocene age (ca. 45 Ma) by identification of gastropods (Nutt and Good, 1998). These sedimentary rocks crop out only rarely along the edges of the Mooney basin and on the east side of Alligator Ridge; they were deposited on Devonian-Mississippian Pilot Shale, Mississippian Joana Limestone, or Mississippian Chainman Shale (Fig. 5). Small outcrops of these rocks are present north of the Yankee deposit, in a pit at the Vantage deposit at Alligator Ridge, and east of the Saga deposit. Conglomerates consist of angular to rounded boulders to pebbles of Diamond Peak Formation, Chainman Shale, Pilot Shale, Joana Limestone (especially chert), or clay-altered igneous rock, and thus, provide an indication of the units exposed in the Eocene, and therefore, the level of erosion. The matrix is calcareous with quartz and chert grains reworked from sandstone, but east of Saga it also includes 2- to 5-mm clear, rounded quartz grains derived from Jurassic porphyry intrusive rocks. The Eocene sedimentary rocks are correlative with the White Sage Formation in the Deep Creek Mountains, Nevada and Utah (Potter et al., 1995), and with the upper part of the Sheep Pass Formation (Good, 1987). To the south, Gans (2000) correlated exposures of lacustrine limestone, siltstone, and sandstone in the northern White Pine Range with the Sheep Pass Formation. The Eocene rocks of the district also may be correlative with the Paleogene Elko Formation, which was deposited in a lacustrine environment on the west side of the uplifted east Humboldt Range-Ruby Mountains core complex (Solomon et al., 1979).

In the north part of the Alligator Ridge district, friable volcaniclastic sandstone is exposed in the Mooney basin and overlies the Galaxy deposit. This rock overlies 36.5 to 34 Ma volcanic rocks, contains abundant clasts of local volcanic rocks, and is considered late Paleogene to Neogene in age and thus unrelated to Eocene sedimentary rocks.

Eocene intrusive rocks are limited to rare dikes in the north part of the Alligator Ridge district; regional aeromagnetic data do not indicate a buried pluton (Ponce, 1991; Grauch, 1996). Deep drill holes about 1 km west of the Yankee deposit and in one of the Yankee pits did not encounter gold mineralization or igneous rocks (Hulen and Collister, 1999; Placer Dome North America, Inc., unpub. data, 2002). The drill hole in the Yankee pit was about 2 km deep (Hulen et al., 1994).

Eocene structure

Eocene structures in the Alligator Ridge district formed at the same time as extension throughout the eastern Great basin, as described above. In the East Humboldt Range-Ruby Mountain core complex to the north of the district, a minimum

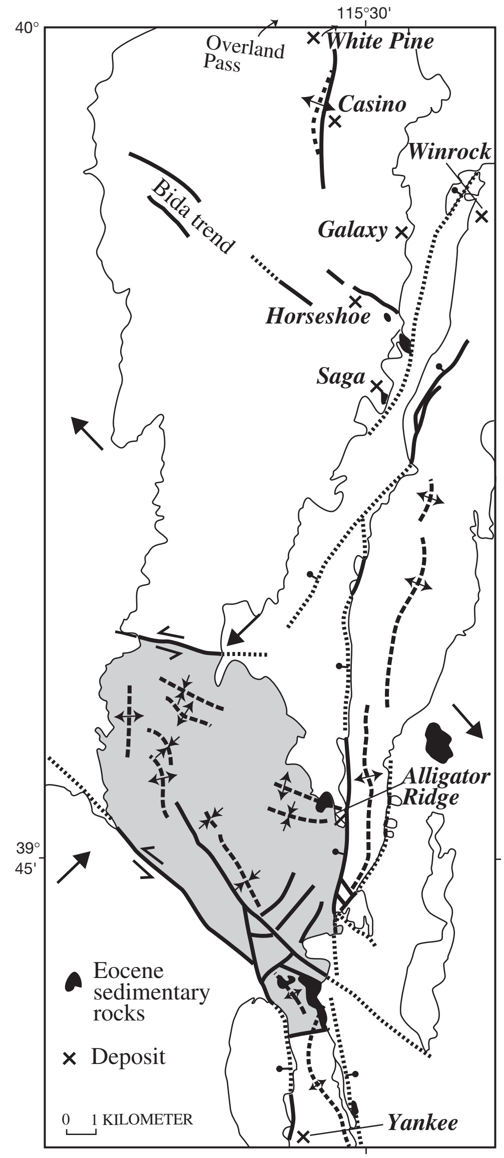

FIG. 5. Eocene structure, sedimentary rocks, and deposits. Deposits shown by ×; Eocene sedimentary rocks in black. Gray area was rotated counterclockwise between west-northwest-striking left-slip faults. Eocene-age folds are in rotated area. Arrows show directions of extension (NW-SE) and compression (NE-SW).

of 7 km of uplift of the core complex during the Late Cretaceous to Paleogene was controlled by a fault on the west side of the complex that displaced rocks to the west-northwest (Howard, 1992; McGrew et al., 2000). Thus, the Alligator Ridge district is south and slightly east of the area of greatest extension but contains structures related to the uplift.

In the Alligator Ridge district, Eocene deformation included development of a basin in which Eocene sediments accumulated, followed by small-amplitude folding, vertical-axis rotation, as well as strike-slip and normal faulting. The basin was nearly coincident with the present-day Mooney basin and was controlled by the Mooney Basin fault system. Following sediment deposition, and prior to 36.5 to 34 Ma volcanism, an episode of deformation caused small-amplitude northwest-trending folding and rotation in the eastern part of the district. The rotation and folds can be explained by left slip along west- to northwest-striking faults (Fig. 5) during uplift of the Ruby Mountains to the north. The north-striking crustal-scale Mooney Basin fault system, however, had normal movement and was the eastern boundary of the rotating block. The largest deposits, Vantage and Yankee, are near the tip of the Mooney Basin fault system, which opened during northwest-southeast extension.

Gold Deposits

The gold deposits in the Alligator Ridge district have been described previously by Klessig (1984), Ilchik et al. (1986), Tapper (1986), Ilchik (1990a), Howald (1996), Stout (1996), Hulen and Collister (1999), and Nutt et al. (2000). Although the deposits have some distinctive features, they are considered to be Carlin-type deposits (Ilchik, 1990a; Hofstra and Cline, 2000; Nutt et al., 2000). The main characteristics of the deposits are summarized in Table 1.

The Alligator Ridge district is about 5 km wide and 40 km long and contains more than 30 small open pits and numerous prospects distributed along or near the Mooney Basin fault system. Total oz Au, mined and in reserves, in the district is 1.44 Moz. Most ore in the district is in carbonaceous calcareous and dolomitic siltstones in the lower part of the Pilot Shale, just above the contact with the Guilmette Formation (Fig. 4). Also, ore locally is in the top of the underlying Guilmette Formation and in the overlying Joana Limestone and lower Chainman Shale. No ore is present in sedimentary rocks younger than the Chainman Shale and all the gold is confined to a stratigraphic interval of 250 m. Local ore controls are anticlines and the intersections of northeast- and northwest- to west-striking faults (see fig. 7 in Nutt et al., 2000). Each deposit shown in Figure 2b consists of one or more pits. Herein, the Alligator Ridge district includes all of the deposits; the Alligator Ridge deposit includes the Vantage I through IV and Luxe pits. The largest (787,500 oz Au) and highest grade (4 ppm Au) deposit was at Alligator Ridge where ore was mined from eight pits. In contrast, 281,284 oz of Au at an average grade of 1.4 ppm Au was extracted from 13 pits at the Yankee deposit. Most gold production has been from oxide ore. Due to the depth of the orebodies and high cost of mineral processing, only the highest grade carbonaceous and sulfidic refractory ores in the Vantage and Winrock deposits were economic. Mineral paragenesis and alteration

TABLE 1. Characteristics of Carlin-Type Gold Deposits in the Alligator Ridge District, Nevada

Characteristic	Alligator Ridge Carlin-type
Mining	Contemporary, disseminated Au
Areal extent of mineralization	5 × 40 km
Number of deposits-pits	More than 30
Contained gold	1.44 Moz
Average Au grade	1.6 g/t
Ore type mined	Mainly oxide, minor carbonaceous
Arrangement of deposits	Distributed along fault system
Deposit form	Irregular strata bound
Structural controls	Mooney basin: north-striking fault system; intersections with NE and NW faults, anticlines, and erosional windows through Chainman Shale cap rock
Stratigraphic controls	Shale-limestone contacts
Stratigraphic interval of mineralization	~250 m
Depth of formation	<300–800 m
Host rocks	Devonian-Mississippian sedimentary rocks, mainly lower Pilot Shale; Jurassic intrusive rock at Horseshoe (see text)
Age of mineralization	Late Eocene: after ca. 45 Ma fluvial and lacustrine sedimentary rocks, before 35–34 Ma volcanic rocks (see text)
Relation to magmatism	Older than local 35–34 Ma magmatism (see text)
Alteration	Silicification, decalcification, argillic (illite, smectite, kaolinite), sulfidation (pyrite, marcasite), maturation of carbonaceous material, incipient graphitization is evident by ability of carbon to rob Au from cyanide solutions
Jasperoid form and distribution	Abundant, mostly concordant to bedding, shallow to moderate depth
Jasperoid grain size	2–200 μm
Jasperoid textures	Shallow: jigsaw mosaic and feathery chalcedonic (T=180°–100°C); deeper: saccharoidal (T >180°C) (see text)
Jasperoid open space filling minerals	Drusy quartz (<1–2 mm) or chalcedony, stibnite, kaolinite, barite
Ore-related minerals	Quartz, calcite, barite, pyrite, marcasite, realgar, orpiment, stibnite, pyrobitumen
Postore open-space-filling minerals	Calcite with petroleum fluid inclusions, oil
Supergene features	Fe oxides, argillic alteration, alunite, jarosite; karst with spelean calcite
Geochemistry	Au/Ag~1 in carbonaceous ore, but locally as high as >20 in oxide ore; enriched in Si, S, As, Sb, Tl, Hg, ± Ba, minor Fe; not enriched in base metals
Fluid inclusions (F.I.)	Calcite: aqueous liquid-rich, T_h = 200°–230°C (see text)

Based mainly on information in Ilchik et al. (1986), Tapper (1986), Ilchik (1990a, b), Hulen and Collister (1999), Nutt et al. (2000), and this study studies in the district have been hampered by the deep and pervasive weathering and oxidation of the ores. Thus, the descriptions of the ores rely heavily on previous studies of unoxidized material (e.g., Ilchik, 1990a) and on our studies of samples obtained from scattered exposures in the pits and drill cuttings collected during the course of this investigation.

Eocene reconstruction and depth of mineralization

The depth of mineralization was reconstructed for the late Eocene, because early to middle Eocene (ca. 45 Ma) conglomerates were silicified by the same fluids that formed the gold deposits (see below), whereas overlying late Eocene to early Oligocene (36.5–34 Ma) rhyolite and intermediate flows were not altered by hydrothermal fluids.

The depth of mineralization was calculated by adding the thickness of Devonian-Mississippian rocks between the deposits and the Eocene paleosurface (= 250 m) and the thickness of Eocene rocks present at the time of mineralization. In the Alligator Ridge area, the thickest section of Eocene sedimentary rocks is at the Vantage 1 pit, where they are about 30 m thick. These 30 m were added to the depth from the Eocene paleosurface in the Chainman Formation to the deposits in the lower Pilot Shale (~75 m of Chainman Formation, 30 m of Joana Limestone, and 150 m of Pilot Shale) to give a maximum depth of formation of about 300 m; however, because Eocene sedimentary rock exposures are small, scattered, and eroded, we also calculated a depth at Alligator Ridge using the thick section of Eocene (?) sedimentary rocks exposed near the Illipah deposit (Fig. 2a) in the northern White Pine Range (Gans, 2000). In this calculation, we used the thickness of the Paleogene Sheep Pass Formation and underlying conglomerate, sandstone, and mudstone (as much as 300 m) as well as the lower part of an overlying section of lacustrine limestone and tuffaceous sedimentary rocks, which includes a 38.1 Ma rhyolite tuff (~200 m), for a total thickness of pre-36 Ma Paleogene rocks of 500 m. If this thick section of Paleocene and Eocene rocks overlaid the Paleozoic rocks that host the Alligator Ridge deposits but was eroded prior to deposition of ca. 36 Ma tuffs, the maximum depth of formation at Alligator Ridge would have been 800 m (500 m of Paleogene rocks and up to 300 m of Paleozoic rocks). Therefore, the depth of formation of the Alligator Ridge deposits is estimated to be ≤300 to 800 m. At the Illipah deposit (Fig. 2a), where gold ore is in the lower Chainman Shale, basal silicified Eocene (?) conglomerate crops out about 200 m above the orebody, so that an addition of about 500 m of Paleogene strata yields a maximum depth for gold deposition at this site of about 700 m (Fig. 6).

Breccias

Breccias are common in the district, host ore in deposits, and have distinctive characteristics which suggest that they formed at different times by different processes. On the district scale, strata-bound jasperoids commonly exhibit a remnant breccia fabric of small angular fragments that predated silicification. In many places, these jasperoids were also affected by later stages of brecciation. The strata-bound jasperoid breccias are localized at the Guilmette Formation-Pilot Shale contact and in the Joana Limestone. In the Horseshoe deposit, Jurassic dike fragments are present in these strata-bound breccias that are variably silicified. At the Vantage deposit, Ilchik (1990a, b) described crackle and mosaic breccias in the lower part of the Pilot Shale and was able to trace stratigraphy through some of them. We observed that some of

FIG. 6. View looking east of the Illipah open pit (foreground, with about 6 m benches) and ridge (horizon, about 1,000 m distant) capped by silicified Eocene conglomerate ~20 m thick. Recognized by Gans (2000) as Permian to Eocene in age and interpreted herein as Eocene because of the similarity to Eocene conglomerate along the Mooney basin. Inset is a close-up of the conglomerate. Similar relations were documented by Nutt et al. (2000) in the Alligator Ridge district.

these breccias are pervasively silicified. In contrast, Tapper (1986) noted dikelike bodies of heterolithic breccias in the Vantage deposit that locally contain rounded clasts, vertically (60 m) transported clasts of Guilmette jasperoid, streaming textures, and a rock flour matrix (e.g., see fig. 14 in Tapper, 1986). Some of the jasperoid breccias in the deposits are cemented by drusy quartz ± stibnite ± barite and others are cemented by supergene alunite dated at 3.6 to 12.4 Ma, jarosite, and/or spelean calcite (Tapper, 1986; Ilchik, 1990a; Arehart et al., 1992; this study). Large karst caverns partially filled with clay and silt were encountered in limestones below jasperoid at the top of the Guilmette Formation at the Yankee and White Pine mines.

Breccias are interpreted as forming by faults, collapse, and/or explosion. The strata-bound jasperoid breccias are attributed to silicification of tectonic breccia zones produced by near bedding-parallel slip between rocks of different competency that probably formed during the large-scale folding event. Slip was concentrated along the contact between thick-bedded Guilmette Limestone and thin-bedded Pilot Shale and in the thin-bedded Joana Limestone, which is between the ductile Pilot and Chainman Shales. Nutt (2000) documented this slip on the district scale. Ilchik (1990a, b) suggested that breccias in which he could trace stratigraphy formed by dissolution and collapse during and after mineralization. Tapper (1986) interpreted dikelike breccia bodies with rounded fragments, vertically transported clasts, and streaming textures as explosion breccias. We interpret the breccias cemented by drusy quartz to be pre- or synore, because the oxygen isotope compositions of drusy quartz are similar to those of gold-bearing jasperoid (see below). The breccias cemented by supergene alunite and spelean calcite and the large karst caverns are postmineralization and late Miocene or younger.

Jasperoids

Jasperoids have been sampled throughout the district (Ilchik, 1990a; Nutt et al., 2000; this study). Compared to other Carlin districts, jasperoids in the Alligator Ridge district are laterally more extensive, extend into Eocene sedimentary rocks, and in the Pilot Shale, Joana Limestone, and Eocene conglomerate, they are finer grained. In the Pilot Shale, decalcified and silicified rocks are associated with ore, whereas in the underlying Guilmette Formation and overlying Joana Limestone, silicified rock often extends well beyond ore zones (Ilchik, 1990a). However, Eocene conglomerates are silicified only where the underlying Joana Limestone or Pilot Shale also are silicified. This relationship is observed near two deposits in the Alligator Ridge district, north of Yankee and east of Saga, and east of the Illipah mine in the White Pine Range (Gans, 2000). Some of these outcrops previously were mapped as jasperoid breccia or sinter rather than as silicified conglomerate. Jasperoids in Eocene conglomerate are barren with 5 to 32 ppb Au, but they contain as much as 447 ppm As, 26 ppm Sb, 24.5 ppm Hg, and 5.6 ppm Tl. Their trace element signature is similar to that of ore (Table 2), hence they may have precipitated from gold-depleted ore fluids.

The jasperoids show a variety of textures defined by Dong et al. (1995). In the Guilmette Formation, the jasperoids have saccharoidal crystalline quartz textures and are relatively coarse grained (10–200 μm); open fractures are lined with drusy quartz (up to 2 mm) ± stibnite, kaolinite, or barite. In contrast, jasperoids in the Pilot Shale, Joana Limestone, and Eocene conglomerate are finer grained (2–50 μm) and commonly have jigsaw mosaic or feathery chalcedonic textures (Fig. 7); fractures are lined with either fine-grained drusy quartz (<500 μm) or banded chalcedony. The jigsaw mosaic and feathery chalcedonic quartz textures are inferred to form by recrystallization from an amorphous silica precursor (Dong et al., 1995) and indicate that the hydrothermal fluids locally were supersaturated with quartz. Cooling below temperatures of 180° to 200°C typically leads to quartz supersaturation (Fournier, 1985; Rimstidt, 1997), but amorphous silica will not precipitate until it reaches saturation at much lower temperatures (Simmons and Browne, 2000), at which point it precipitates in large amounts. For example, a 230°C quartz-saturated solution would have to cool to 100°C before amorphous silica saturation is reached. Thus, the crystalline quartz in Guilmette Formation jasperoids may have formed at temperatures greater than 180° to 200°C. Conversely, the jasperoids with textures inherited from an amorphous silica precursor may have precipitated or recrystallized at low temperatures of between 180° and 100°C.

Mineralogy and Geochemistry

The deposits have average Au grades of <4 ppm. The Au/Ag ratios of oxide ores range from >20 at Alligator Ridge to 0.3 at the Yankee deposit and average close to 1 (Ilchik, 1990a; Table 2). Because the carbonaceous ores at Alligator Ridge have Au/Ag close to 1 (Ilchik, 1990a), we infer that much of the variability in Au/Ag ratios is due to variable Ag depletion associated with weathering and supergene oxidation of the ores. Table 2 shows that all deposits from Yankee in the south to White Pine in the north have similar geochemical signatures, showing enrichments in As, Sb, Hg, and Tl.

TABLE 2. Downhole Geochemistry from Deposits in the Alligator Ridge District (in ppm)

Deposit	Host	Hole	Feet	Au	Ag	As	Sb	Hg	Tl	Cu	Pb	Zn	Mo	Bi	Te	Sn
Alligator Ridge	MDp/Dg	VVD-8	720–820	4.10	<0.2	1,135	48	9.0	6.3	26	15	267	25	<1	<0.02	<20
Yankee	MDp/Dg	YX-1	430–510	0.97	2.90	329	64	3.0	2.0	13	5	23	5	<1	<0.02	<20
Galaxy	MDp/Dg	GXR-229	290–340	1.67	0.16	938	152	28.8	10.2	27	27	92	15	<1	<0.02	<20
Saga	MDp/Dg	SGR-222	160–240	0.92	<0.2	298	101	3.3	4.7	45	24	96	31	<1	<0.02	<20
Horseshoe	MDp/Dg	EBQ-045	270–330	0.44	<0.2	379	127	20.7	31.4	20	20	88	13	<1	<0.02	<20
Casino	MDp/Dg	CR-157	50–80	1.37	0.3	618	180	<32	<49	21	29	37	8	<1	<0.02	<20

Values for Alligator Ridge from drilled Pentium resource east of Vantage; values are average of intervals; samples from Alligator Ridge from unoxidized ore; other deposits from oxidized ore; no data from Winrock and White Pine

Abbreviations: MDp = Pilot Shale; Dg = Guilmette Formation

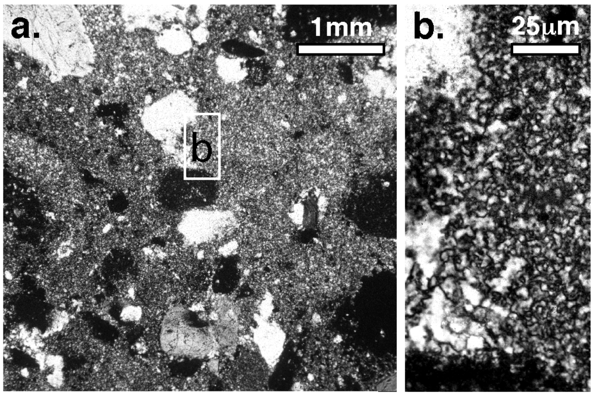

FIG. 7. Photomicrograph of silicified Eocene sandstone. a. A variety of clast types in cross-polarized transmitted light. b. Closeup of jigsaw mosaic texture quartz in the matrix of (a).

Mineralogy

Native gold has been observed only in or on limonite in oxide ores (Tapper, 1986). Electron microprobe analyses and SEM studies show that decalcified carbonaceous ores contain disseminated arsenian pyrite and marcasite. Based on studies of other Carlin-type deposits (Hofstra and Cline, 2000), these minerals are probable hosts for the gold. In many places, the carbonaceous ores and adjacent rocks contain ore-stage orpiment or realgar in fractures with calcite, and locally, pyrite, marcasite, or barite. Illite is the predominant phyllosilicate in unoxidized carbonaceous ores (Ilchik, 1990a), but in strongly altered ore-grade samples we observed smectite and kaolinite in close association with arsenian pyrite overgrowths on diagenetic framboidal pyrite (Fig. 8). Kaolinite, along with stibnite, also is present in drusy quartz veinlets in jasperoid (Ilchik, 1990b). In addition, the low K_2O/Al_2O_3 of carbonaceous ore samples (see fig. 7d in Ilchik, 1990a) suggests the presence of about 10 wt percent kaolinite or smectite. Carbonaceous ores also have Fe_2O_3/Al_2O_3 and TiO_3/Al_2O_3 that are about 10 percent higher than those of unaltered rocks, suggesting that there may have been minor Fe introduction.

The presence of marcasite may be interpreted to indicate temperatures of <240°C and pH <5 (Murowchick, 1992). Low pH is also suggested by the presence of kaolinite in veinlets and in ore. Orpiment and realgar form at low temperatures and moderate to high sulfidation states (Hofstra and Cline, 2000).

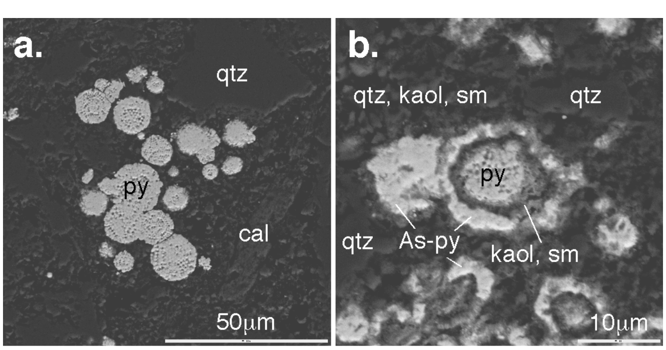

FIG. 8. a. Pyrite framboids in barren calcareous shale. b. Arsenian pyrite rims on pyrite framboids in decalcified and argillically altered shale. As-py = arsenian pyrite; cal = calcite; kaol = kaolinite; qtz = quartz; sm = smectite.

The greater abundance of disseminated arsenian pyrite and marcasite in carbonaceous ores relative to unaltered wall rocks and the minor Fe introduction suggest that sulfidation of host-rock Fe and mixing with Fe-bearing ground water were important precipitation mechanisms (Hofstra and Cline, 2000).

Thermal maturity parameters

The deposits at Alligator Ridge contain indigenous kerogen and introduced pyrobitumen. Based on Rock Eval pyrolysis and reflectance measurements, the kerogen in the ore is substantially more mature than that in barren rocks distal to the ore (Ilchik et al., 1986). The low maturity of kerogen in the Pilot Shale outside the deposits is consistent with a conodont CAI (Color Alteration Index) of 1.5 in the Joana Limestone that corresponds to a temperature <90°C and a burial depth <3 km (Anita G. Harris, written commun., 2001). At Yankee, ore-related calcite-realgar-marcasite veins contain blebs of highly reflective pyrobitumen (Nutt et al., 2000). Given that oil is fully cracked to pyrobitumen and methane at temperatures of about 150° to 200°C (Hunt, 1996; Hulen and Collister, 1999), the presence of pyrobitumen in these veins suggests that similar or greater temperatures were attained during gold mineralization. In contrast, postore calcite at Yankee contains liquid petroleum inclusions and oil is present in fractures and pores. This petroleum exhibits biomarker transformations indicative of temperatures between 113° and 146°C (Hulen and Collister, 1999). Our interpretation that the calcite with liquid petroleum inclusions is postore, as well as the paragenetic relationships upon which it is based (Fig. 9), contrasts with that of Hulen and Collister (1999), who interpreted the calcite with petroleum inclusions as ore related.

Fluid inclusions

Petrographic observations and crushing studies of fluid inclusions were conducted to facilitate interpretation of microthermometric data in Ilchik (1990b) and Hulen et al. (1994). Ore-stage calcite contains aqueous, liquid-rich fluid inclusions that have fairly constant phase ratios suggesting that they were trapped in the one-phase field. A few of the larger inclusions have homogenization temperatures of 200° to 230°C (Ilchik, 1990b). By analogy with results from similar well-studied systems, these inclusions probably also contain some salt and CO_2; however, our crushing studies of ore-related calcite in oil (e.g., Bodnar et al., 1985) produced nil to extremely small vapor bubbles, consistent with low gas contents. The range of homogenization temperatures indicates a minimum depth of trapping between 160 to 600 m under lithostatic and hydrostatic pressures, respectively, assuming a salinity of 3 wt percent similar to that of other Carlin-type deposits (Hofstra and Cline, 2000) and a low CO_2 content (e.g., ≤0.37 mole %; Bodnar et al., 1985). These depths are consistent with our reconstruction. Postore calcite at Yankee (Nutt et al., 2000) contains both petroleum and aqueous fluid inclusions with low homogenization temperatures between 50° and 150°C and salinities less than 3.55 wt percent NaCl equiv (Hulen et al., 1994).

Stable Isotopes

The oxygen, hydrogen, carbon, and sulfur isotope data in Ilchik (1990a, b) are plotted together with our data (Table 3) in Figures 10 to 12 and summarized in Tables 4 and 5.

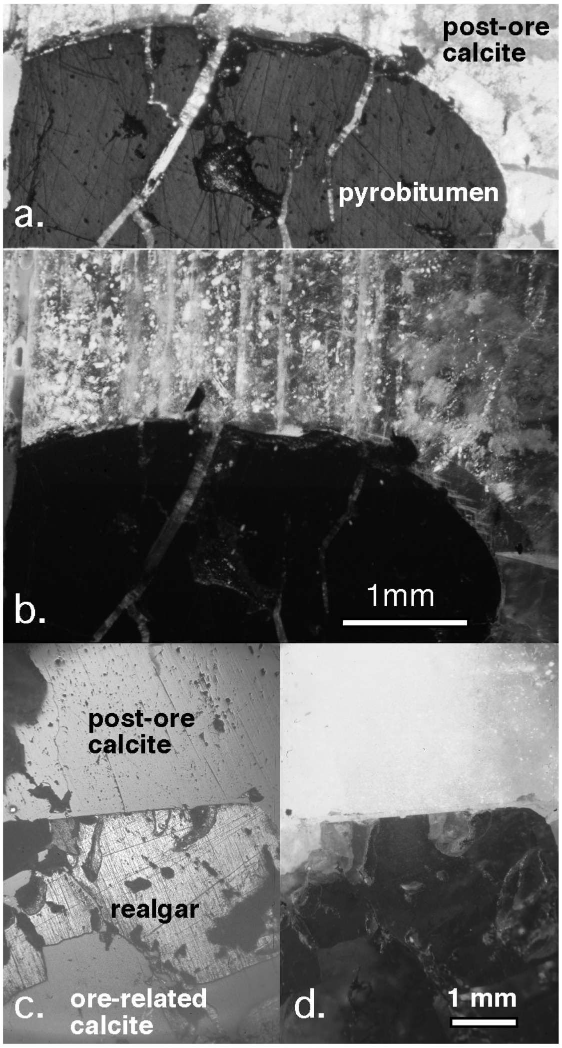

FIG. 9. Ore-related calcite, realgar, and pyrobitumen on vein walls mantled by postore calcite containing petroleum inclusions, Yankee deposit. a. Reflected and transmitted light photomicrograph of highly reflective, fractured pyrobitumen cemented and mantled by postore calcite. b. Same sample as (a) under ultraviolet light. Note fluorescent petroleum inclusions in postore calcite. c. Reflected light photomicrograph of ore-related calcite and realgar mantled by postore calcite. d. Same view as (c) under ultraviolet light. Note the abundance of fluorescent petroleum inclusions in postore calcite and paucity of these inclusions in ore-related calcite and realgar.

Oxygen and hydrogen isotopes of quartz and kaolinite

The $\delta^{18}O$ values of jasperoid and drusy quartz veinlets are shown in Figure 10 and Table 5. The $\delta^{18}O$ values of jasperoid in the Eocene conglomerates are similar to those in underlying Devonian-Mississippian rocks and are similar to those of ore-grade jasperoid and drusy quartz veinlets in the Pilot Shale, where most ore resides. These similarities suggest that barren and ore-grade jasperoids in all of these rock units were deposited from the same fluids in the late Eocene. The ~12 per mil range of $\delta^{18}O$ values, with a mode of 17 per mil, reflects a combination of cooling, mixing, recrystallization, and exchange with host rocks. Cooling from a peak temperature of 230° to 100°C can account for 11 per mil of this range and is consistent with the fluid inclusion data and jasperoid textures. The remaining variation may be due to mixing with surficial meteoric water ($\delta^{18}O$ = –16‰; calculated from δD values of Ilchik, 1990b, and the meteoric water line), exchange between amorphous silica and pore fluids during recrystallization over a range of temperatures, exchange with sedimentary host rocks (carbonates and siltstones $\delta^{18}O$ = 20–25‰, chert $\delta^{18}O$ = 24–29‰; from Ilchik, 1990b, and this study), and/or samples that contain relict material from the host rocks.

Because jasperoids with different textures, in different host rocks, at different levels in the system have the same range of $\delta^{18}O$ values, the modal value of 17 per mil and temperatures of 230° to 100°C were used to calculate a range of $\delta^{18}O_{H2O}$ values of –4 to 7 per mil using the quartz-H_2O fractionation in Zheng (1993). The δD_{H2O} values were calculated at 200°C based on kaolinite δD values of –116 to –106 per mil from drusy quartz-stibnite-kaolinite veinlets (Ilchik, 1990b; Hofstra et al., 1999) using the kaolinite-H_2O fractionation in Sheppard and Gilg (1996). Together, these data indicate that the hydrothermal fluids were meteoric in origin and shifted about 13 to 23 per mil from the meteoric water line (Fig. 11). Such large isotopic shifts indicate that the hydrothermal fluids originated from reaction of meteoric water with sedimentary source rocks at low water/rock ratios (1 to 0.1) and elevated temperatures (>200°C).

Carbon and oxygen isotopes of carbonate minerals

Altered rocks and calcite veins are shifted to lower $\delta^{18}O$ and higher $\delta^{13}C$ values relative to fresh rocks (see fig. 10 in Ilchik, 1990a), as in some other Carlin-type deposits (e.g., Meikle; Emsbo et al., 2003). The $\delta^{18}O_{H2O}$ and $\delta^{13}C_{CO2}$ values of the hydrothermal fluids were calculated using the calcite-H_2O and calcite-CO_2 fractionation factors of O'Neil et al. (1969) and Chacko et al. (1991), respectively. By pairing the maximum temperature of 230°C with the lowest $\delta^{18}O$ values

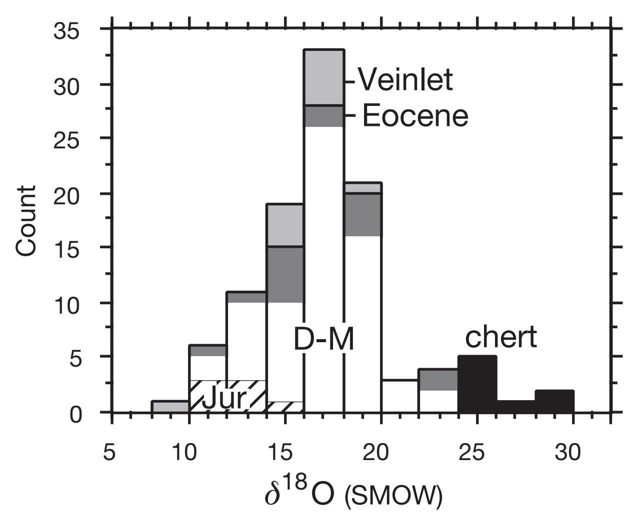

FIG. 10. Histogram of $\delta^{18}O$ values of jasperoids hosted in Devonian-Mississippian rocks (white), Jurassic porphyry intrusion at Horseshoe (hachured), Eocene conglomerate (dark gray), and quartz veinlets in these jasperoids (light gray). Also shown are sedimentary-diagenetic cherts (black) that have higher $\delta^{18}O$ values than those of jasperoids.

TABLE 3. Isotopic Data for Quartz, Sulfides, Barite, and Alunite from the Alligator Ridge and Illipah Districts, Nevada

Sample no.	Deposit/location	Host rock	Comment	Mineral	$\delta^{34}S$ (‰)[1]	$\delta^{18}O$(‰)[2]
Alligator Ridge						
98-YEJ	N. of Yankee	Eocene sandstone	Barren	Drusy quartz		18.7
98-YEJ	N. of Yankee	Eocene sandstone	Barren	Jasperoid matrix		22.6
98-YEJ	N. of Yankee	Eocene sandstone	Barren	Jasperoid clast		22.4
99-YEV-Mj	N. of Yankee	Joana Limestone	Barren	Jasperoid matrix, chert breccia		19.1
99-YEJ	N. of Yankee	Eocene sandstone	Barren	Opal veinlet		–1.1
BMAR-00-1	SE of Saga	Eocene conglomerate		Silicified matrix-a		18.8
BMAR-00-1	SE of Saga	Eocene conglomerate		Silicified matrix-b		17.6
BMAR-00-2	SE of Saga	Pilot Shale		Jasperoid		17.1
BMAR-00-3a	SE of Saga	Pilot Shale		Chalcedony veinlet		16.4
BMAR-00-3b	SE of Saga	Pilot Shale		Limonitic, partially silicified		8.5
BMAR-00-4a	E. of Saga	Eocene conglomerate		Matrix		15.0
BMAR-00-4c	E. of Saga	Eocene conglomerate		Matrix-a		15.9
BMAR-00-4c	E. of Saga	Eocene conglomerate		Matrix-b		15.6
BMAR-00-4c	E. of Saga	Eocene conglomerate		Jurassic quartz phenocryst		13.4
BMAR-00-4d	E. of Saga	Eocene conglomerate		Matrix		18.5
BMAR-00-5b	NE of Saga	Eocene conglomerate		Silicified groundmass of intrusion clast		15.7
BMAR-00-6	NE of Saga	Eocene conglomerate		Matrix		17.4
BMAR-00-7	Saga pit	Pilot Shale	Ore	Jasperoid		14.4
HS-00-1Aa	Horseshoe	Jurassic porphyry intrusion	Mid-level	Silicified groundmass		13.8
HS-00-1Ab	Horseshoe	Jurassic porphyry intrusion	Mid-level	Quartz phenocryst		12.0
HS-00-1Ca	Horseshoe	Pilot Shale	Mid-level	Breccia matrix		15.6
HS-00-1Cb	Horseshoe	Pilot Shale	Mid-level	Pilot fragment in breccia		18.0
HS-00-1H	Horseshoe	Pilot Shale	Mid-level	Silicified breccia		15.6
HS-00-2E	Horseshoe	Pilot Shale	Upper bench	Jasperoid		12.2
HS-00-2H	Horseshoe	Jurassic porphyry intrusion	Upper bench	Breccia matrix		13.6
HS-00-2Ka	Horseshoe	Jurassic porphyry intrusion	Upper bench	Silicified groundmass		11.6
HS-00-2Kb	Horseshoe	Jurassic porphyry intrusion	Upper bench	Quartz phenocryst		11.7
GX-00-1Aa	Galaxy	Guilmette Formation		Breccia matrix		16.6
GX-00-1Ab	Galaxy	Guilmette Formation		Guilmette jasperoid fragment		14.5
GX-00-1C	Galaxy	Pilot Shale		Pilot jasperoid fragment		17.2
GX-00-1E	Galaxy	Pilot Shale		Breccia matrix		19.3
GX-00-2Aa	Galaxy	Joana Limestone		Breccia matrix		19.9
GX-00-2Ab	Galaxy	Joana Limestone		Joana jasperoid fragment		15.9
GX-00-3a	Galaxy	Guilmette-Pilot		Milky quartz		16.5
GX-00-3b	Galaxy	Guilmette-Pilot		Dark Pilot chert fragment		25.0
GX-00-3c	Galaxy	Guilmette-Pilot		Drusy quartz		16.7
GX-00-3d	Galaxy	Guilmette-Pilot		Sugary Guilmette fragment		16.9
WR-00-1a	Winrock	Chainman Shale		Jasperoid		11.8
WR-00-5a	Winrock	Joana Limestone		Matrix		8.8
WR-00-5b	Winrock	Joana Limestone		Drusy quartz		10.2
WR-00-6	Winrock	Joana Limestone		Black chert		24.6
97-WC-005	West Crusher	Pilot Shale	Ore	Realgar	12.4	
97-WC-006	West Crusher	Pilot Shale	Ore	Realgar	12.9	
97-WC-002	West Crusher	Pilot Shale	Ore	Realgar	7.7	
97-WC-008	West Crusher	Pilot Shale	Ore	Orpiment	12.2	
97-WC-002	West Crusher	Pilot Shale	Ore	Realgar	8.9	
99-YEJ	N. of Yankee	Eocene sandstone	Barren	Pyrite	–7.7	
Casino-99	Casino	Guilmette Formation		Early barite in jasperoid	39.7	12.9
Vantage-99	Vantage	Guilmette-Pilot		Late barite in jasperoid	25.0	9.4
Casino-99	Casino	Guilmette-Pilot		Late barite in jasperoid	27.6	8.2
Whitepine-99	White Pine	Guilmette Formation		Early barite in jasperoid	36.5	17.0
99-YEV Mj	N. of Yankee	Joana Limestone	Barren	Late barite in jasperoid	25.3	nd
Whitepine-99	White Pine	Guilmette-Pilot		Late barite in jasperoid	34.4	nd
WR-00-3	Winrock	Chainman Shale		Late barite	35.8	2.4
WR-00-6	Winrock	Chainman Shale		Late barite	21.0	–6.2
GX-00-1B	Galaxy	Guilmette Formation		Early barite	21.2	11.0
HS-00-2A	Horseshoe	Guilmette-Pilot contact?	Upper bench	Early barite vein	40.9	11.6
BMAR-00-4A	E. of Saga	Guilmette Formation?		Early barite, jasperoid float	31.0	16.4
BMAR-00-4A	E. of Saga	Guilmette Formation?		Early barite, jasperoid float	28.3	nd
GX-00-4	Galaxy	Guilmette-Pilot breccia		Supergene alunite vein		–5.1
Illipah						
GSN2000-1	E. of Illipah	Joana Limestone	150 m south of Eocene conglomerate	Grayish red jasperoid		12.0
IP-00-1a	E. of Illipah	Eocene conglomerate		Silicified matrix		14.6
IP-00-1b	E. of Illipah	Eocene conglomerate		Silicified matrix		12.2

TABLE 3. (Cont.)

Sample no.	Deposit/location	Host rock	Comment	Mineral	$\delta^{34}S$ (‰)[1]	$\delta^{18}O$ (‰)[2]
IP-00-1c	E. of Illipah	Eocene conglomerate		Silicified matrix		11.4
IP-00-4a	Illipah	Top of Needles Siltstone	East end of pit	Siltstone, limonitic		24.9
IP-00-4b	Illipah	Top of Needles Siltstone	East end of pit	Siltstone, limonitic		23.2
IP-00-5a	E. of Illipah	Joana Limestone	Below Eocene conglomerate	Tan slightly translucent jasperoid		19.9
IP-00-5b	E. of Illipah	Joana Limestone	Below Eocene conglomerate	White jasperoid		15.9
IP-00-6	Illipah	Needles Siltstone, calcareous	Middle of pit, fault	Limonite + partial silicification		3.8
IP-00-4B	Illipah	Needles Siltstone		Late barite	31.2	25.3

All analyses were conducted in R.O. Rye's laboratory at the U.S. Geological Survey in Denver; W.D. Christiansen, analyst; West Crusher is pit at Yankee

[1] The $\delta^{34}S$ compositions of sulfides and sulfates were determined by an on-line method using an elemental analyzer coupled to a Micromass Optima mass spectrometer following Giesemann et al. (1994); analytical precision generally was better than ±0.2‰

[2] The $\delta^{18}O$ compositions of silicates and barite were determined using bromine pentafluoride digestions as described by Clayton and Mayeda (1963) on a Finnigan MAT 252 mass spectrometer

from the veins and a lower temperature of 100°C with the highest $\delta^{18}O$ values, $\delta^{18}O_{H2O}$ values from –4.3 to 2.3 per mil are obtained that are at the lower end of the range calculated for jasperoids (Fig. 10). Similarly, if the veins with the highest $\delta^{13}C$ values formed at the lowest temperature and those with the lowest $\delta^{13}C$ values formed at the highest temperature, then a narrow range of $\delta^{13}C_{CO2}$ values from –0.9 to –0.4 per mil is obtained, which is about average for the carbonate rocks in the area. Thus, the veins with high $\delta^{13}C$ values may reflect precipitation at low temperatures from fluids that previously dissolved carbonate host rocks. Alternatively, the high $\delta^{13}C$ values may be due to reduction of a small proportion of CO_2 to CH_4 by indigenous organic matter during mineralization (Emsbo et al., 2003) or introduction of heavy carbon from an unidentified external source.

TABLE 4. Isotopic Characteristics of Carlin-Type Gold Deposits in the Alligator Ridge District, Nevada

Characteristic	Alligator Ridge Carlin-type
Kaolinite: H isotopes	Kaolinite δD = –122 to –132‰; whole-rock carbonaceous ore (illite) δD = –116 to –119‰ (meteoric water)
Quartz: O isotopes	Jasperoid: $\delta^{18}O$ = 11 to 24‰, mode $\delta^{18}O$ = 17‰; drusy quartz in jasperoid: $\delta^{18}O$ = 10.2 to 20.1‰; chalcedony veinlet in jasperoid: $\delta^{18}O$ = 16.4‰; opal veinlet in jasperoid: $\delta^{18}O$ = –1.1‰ (meteoric water that evolved by exchange with carbonate rocks)
Carbonate: C and O isotopes	Fresh rocks: $\delta^{13}C$ = –2.1 to 2.1‰, $\delta^{18}O$ = 19.8 to 25.5‰; altered rocks: $\delta^{13}C$ = –2.3 to 1.4‰, $\delta^{18}O$ = 12.7 to 25.7 ‰; vein calcite: $\delta^{13}C$ = –1.3 to 3.1‰, $\delta^{18}O$ = 3.8 to 19.4‰ (increased $\delta^{13}C$ values and decreased $\delta^{18}O$ values reflect precipitation of calcite at low temperatures from exchanged meteoric water ± minor reduction of CO_2 to CH_4 by organic matter in the rocks)
Sulfide: S isotopes	$\delta^{34}S$ = –7.7 to 14.4‰ (reduced S leached from sedimentary rocks by exchanged meteoric water)
Sulfate: S and O isotopes	Early barite: $\delta^{34}S$ = 25.9 to 47.1‰, $\delta^{18}O$ = 11.0 to 17.0‰; late barite: $\delta^{34}S$ = 21.0 to 39.4‰, $\delta^{18}O$ = –6.2 to 9.4‰ (late sulfate derived from dissolution of sedimentary sulfate [barite] and oxidation of preexisting sulfide minerals)

Based on data in Ilchik (1990a, b) and Table 3

Sulfur isotopes of sulfides

The $\delta^{34}S$ values of sulfide minerals in the Alligator Ridge district have a wide range (Fig. 12). Diagenetic pyrite in barren Pilot Shale has $\delta^{34}S$ values between –4.5 and 4.4 per mil, mineralized samples containing mixtures of diagenetic and ore-stage pyrite and marcasite have values to 11.6 per mil, and late orpiment, realgar, and stibnite have values that range from –7.7 to 14.4 per mil, with 70 percent of all ore-stage values ≥6.1 per mil. Thus, the higher $\delta^{34}S$ values are most representative of ore fluids, and at temperatures of 230° to 100°C, yield $\delta^{34}S_{H2S}$ values of 11.5 to 17.4 per mil using fractionation factors in Ohmoto and Rye (1979). These $\delta^{34}S_{H2S}$ values are at the high end of the range for Carlin-type deposits (Hofstra and Cline, 2000). Figure 12 shows that H_2S with this range of $\delta^{34}S$ values could have been produced by thermochemical reduction of authigenic barite in the Guilmette Formation ($\delta^{34}S$ = 25.9–47.1‰) or by dissolution of diagenetic pyrite from Cambrian and Late Proterozoic rocks at depth (Ilchik, 1990a). The negative $\delta^{34}S$ values may be due to

TABLE 5. Ranges of Jasperoid Oxygen Isotope Data (‰) for Each Formation in the District and at Three Locations where Eocene Conglomerate and Underlying Formations Are Silicified

Lithology	District	East of Saga	North of Yankee	East of Illipah
Eocene conglomerate	22.6–11.4	18.8–15.0	22.6–18.7	14.6–11.4
Chainman Shale	23.2–11.8	Absent	Absent	Absent
Joana Limestone	20.2–11.6	Absent	19.1	19.9–12.0
Pilot Shale	20.1–12.2	17.1–14.4		
Guilmette Formation	20.1–12.9			
Jurassic porphyry	15.7–11.6			
Veinlets	20.1–10.2			
Mode	17.0			

Data from Ilchik (1990b) and Table 3

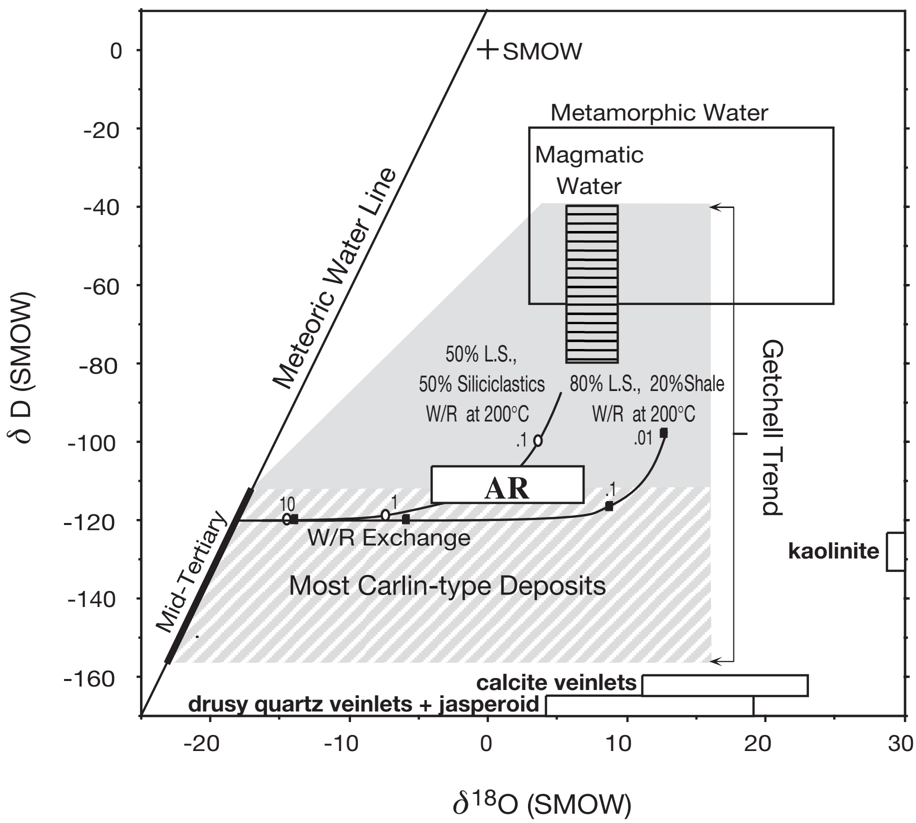

FIG. 11. Calculated δD and $\delta^{18}O$ compositions of ore fluids at Alligator Ridge (AR) based on δD analyses of kaolinite in quartz-stibnite-kaolinite veinlets (vertical bar; Ilchik, 1990b) and $\delta^{18}O$ data from drusy quartz veinlets and jasperoid and ore-related calcite veinlets (horizontal bars; Ilchik, 1990a; Table 3). Range of fluid compositions found in most Carlin-type Au deposits (gray hachured area) and in the Getchell trend (gray triangular area + hachured area) are from Hofstra and Cline (2000). L.S. = marine limestone, W/R = water/rock. See text for further description.

low-temperature oxidation, with formation of metastable sulfur species, and/or bacterial sulfate reduction during the waning stages of the hydrothermal system (perithermal environment of Plumlee and Rye, 1992) or due to mixing with an external fluid containing light sulfur, such as local ground water.

Sulfur and oxygen isotopes of barite

Paragenetic relations in jasperoids show that barite deposition was both early, prior to silicification, and late, after silicification and the formation of drusy quartz. The early barite has textures suggesting that it is authigenic; in contrast, the late barite fills open fractures and vugs. The $\delta^{34}S$ values of early barite in the Guilmette Formation range between 25.9 and 47.1 per mil (avg 35.9‰), whereas those of late barite range between 21.0 and 39.4 per mil (avg 26.4‰). Early barite has $\delta^{18}O$ values between 11.6 and 17.0 per mil and late barite values from –6.2 to 11.0 per mil (Fig. 12). The $\delta^{34}S$ and $\delta^{18}O$ values of early barite are the same or greater than those of Late Devonian sedimentary exhalative barite throughout Nevada (Papke, 1984), and the higher values are consistent with the sulfur isotope shifts produced by closed-system bacterial reduction of sulfate (Ohmoto and Rye, 1979).

Late barite precipitated after ore-related minerals but before supergene alunite, and it thus formed either during the latest stages of the hydrothermal system or is postore. The $\delta^{34}S$ and $\delta^{18}O$ values of late barite are intermediate between those of the early barites and sulfate that would be generated by oxidation of H_2S- bearing fluids or sulfide minerals by meteoric water. Thus, the sulfate in late barite is probably a mixture derived from the two end members. The late barite sample with the lowest $\delta^{18}O$ value of –6.2 per mil must have formed almost exclusively by the oxidation of preexisting sulfide minerals by meteoric water. If late barite is ore related, the oxidation it records is consistent with a shallow environment.

Distinctive Features of the Alligator Ridge District

In comparison with other Carlin-type gold districts in Nevada (see Hofstra and Cline, 2000), the Alligator Ridge district is distinctive in the following ways: (1) the deposits are smaller, lower grade, and have lower Au/Ag ratios; (2) stratigraphic reconstructions indicate that the deposits formed at shallow depths; (3) the cap rock consists of conformable Chainman Shale rather than the Roberts Mountains allochthon; (4) in areas where this cap rock was absent, basal Eocene conglomerate and sandstone are silicified; (5) the organic matter in the host rocks was relatively immature and susceptible to alteration; (6) mineralization predates local late Eocene igneous activity; (7) jasperoids are more extensive and voluminous and some have feathery chalcedonic and jig-

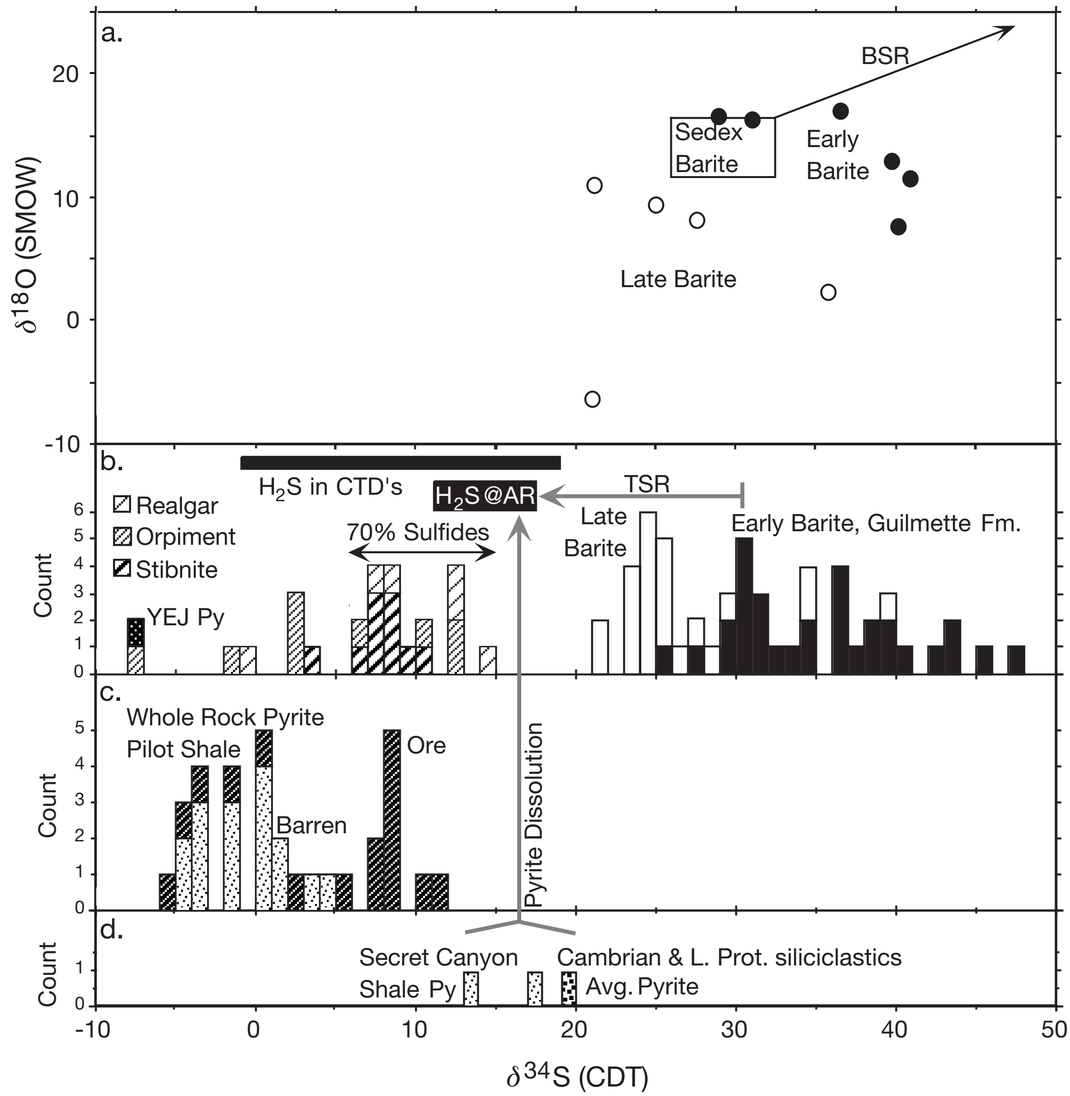

FIG. 12. a. δ^{34}S and δ^{18}O isotopic compositions of early and late barite relative to the field for Devonian sedimentary exhalative (Sedex) barite in Nevada (Papke, 1984) and closed-system bacterial sulfate reduction (BSR) trajectory (Rye et al., 1978; Cecile et al., 1983). b. Histograms of δ^{34}S data for early barite, late barite, and ore-related open-space-filling sulfide minerals (Ilchik, 1990a; Table 3). YEJ Py = pyrite in Eocene-hosted jasperoid north of the Yankee deposit. Seventy percent of the ore-related sulfides have δ^{34}S values >6.1 per mil. The black bar shows the corresponding calculated values for H_2S in ore fluids relative to the full range (gray bar) in Carlin-type deposits (CTD's) (from Hofstra and Cline, 2000). c. Histograms of whole-rock δ^{34}S data on barren and ore-grade Pilot Shale (from Ilchik, 1990a). d. δ^{34}S values of pyrite (py) in Cambrian Secret Canyon shale (Hitchborn et al., 1996) and average values for Lower Cambrian and Late Proterozoic siliciclastic rocks (Vikre, 2000). The horizontal and vertical gray arrows show that H_2S in ore fluids was most likely generated by thermochemical reduction of early barite (TSR) and/or by dissolution of diagenetic pyrite in underlying Cambrian and Late Proterozoic (L. Prot.) rocks. AR = Alligator Ridge.

saw mosaic textures which suggest that they recrystallized from an amorphous silica precursor; and (8) the δ^{18}O values of barren and mineralized jasperoid are higher than those in other districts.

The available data suggest that the deposits and related jasperoids in the Alligator Ridge district formed in the late Eocene, at shallow depths of 800 m or less, at temperatures between 230° and 100°C, from dilute, moderately acidic, reduced, H_2S-bearing meteoric fluids. These fluids transported significant Si, S, Au, Ag, As, Sb, Hg, Tl, and Ba, but little Fe or base metals. Ore fluids ascended along permeable channels in the Mooney Basin fault system until they encountered impermeable strata, at which point they moved laterally through permeable and reactive strata in the Guilmette Formation, Pilot Shale, and Joana Limestone toward erosional windows where they ascended into Eocene fluvial conglomerates.

Considering the absence of a local coeval magmatic center, a different driving mechanism for fluid movement must have been present. The thermal energy required to drive fluid movement may have come from Eocene regional magmatism and/or increased thermal gradients related to crustal thinning during large-magnitude extension in the core complexes (Ilchik and Barton, 1997; Hofstra et al., 1999). Either mechanism would have increased fluid temperatures and promoted convection in the Mooney Basin fault system. However, the direction of fluid flow during extension of the East Humboldt-Ruby Mountains core complex depended on the amount of topographic relief in the complex. For example, if topographic relief were low, fluid flow would have been toward and above the complex, whereas if topographic relief were high, fluid flow would have been down and away from the complex. A tenable hypothesis is that fluid flow was gravity driven with recharge in the uplifted core complex and south-directed fluid flow focused along the dilatant Mooney Basin fault system into the adjacent Alligator Ridge district. If geothermal gradients were near 30°C/km and peak fluid temperatures were near 230°C, then ore fluids came from depths = 8 km, which is consistent with the high $\delta^{18}O$ values of the fluids. On the basis of δD compositions and $^{40}Ar/^{39}Ar$ cooling dates on biotite, Wickham et al. (1993) present independent evidence for circulation of meteoric water to the brittle-ductile transition at depths of 10 to 12 km in the East Humboldt Range-Ruby Mountains core complex at >32 Ma,

Gold was transported as a bisulfide complex (Hofstra et al., 1991) and the H_2S in the fluids was derived from sedimentary rocks as shown by the $\delta^{34}S$ values of ore-stage sulfide minerals. Gold was probably leached from sedimentary rocks, which have similar $\delta^{34}S$ values, at deep levels in the system. If fluids remained undersaturated with Au after their ascent, they may have scavenged additional Au from calcareous clastic rocks in the zones of lateral flow. As in other Carlin-type deposits, auriferous Fe sulfide minerals precipitated by sulfidation (Hofstra et al., 1991; Hofstra and Cline, 2000) and minor mixing with Fe-bearing ground water. Sulfidation took place where Au-saturated or nearly saturated fluids encountered strata containing reactive Fe-bearing minerals; presumably this is one reason that the lower Pilot Shale is the preferred host. Recent hydrothermal experiments by Wilder and Seward (2002) suggest that adsorption of Au from undersaturated solutions onto pyrite is only important under acidic conditions where $AuHS^0$ is the predominant complex. Thus, the acidic conditions, indicated by the presence of kaolinite and marcasite, may have been conducive to gold deposition by this process. As the hot acidic fluids were neutralized by reactions with cool sedimentary rocks, calcite, and locally, dolomite dissolved and amorphous silica or quartz precipitated, with a large proportion of the silica precipitating between the sites of ore formation and outflow zones.

The low Au grade and small size of the deposits suggests that the ore fluids transported less Au than those in the larger Carlin-type districts and/or that host rocks were less effective at fixing Au from these fluids. The large volume of jasperoid in the district, and the modeling calculations that indicate water/rock ratios of about 1,000 are required to replace limestone with quartz at constant volume (Ilchik and Barton, 1997), suggests that fluid flux was high. Therefore, the low Au content of the district is unlikely due to low fluid flux. Chemical modeling shows that lower Au solubilities and lower Au/Ag ratios result as H_2S contents and temperatures decrease (Gammons and Williams-Jones, 1995; A.H. Hofstra, unpubl. data, 2002), both of which would be expected as fluids move to shallow depths where confining pressures are low. The low Au/Ag ratios also may be due in part to the high background abundance of Ag (0.2–5 ppm) in the Pilot Shale (Placer Dome North America, Inc., data) and to the relatively small amount of Au precipitated. Thus, many distinctive features of the gold deposits in the Alligator Ridge district may be attributed to Carlin-type mineralization in a shallow environment.

Note Added in Proof

The concentrations of trace elements in arsenian pyrite (Fig. 8b) from the Winrock deposit were determined by laser ablation-inductively coupled plasma mass spectrometry at the U.S. Geological Survey in Denver using a method similar to that of Ridley (2000). A laser spot size of 10 μm and a linear travel rate of 15 μm/s were used to generate several element profiles across a polished thin section of ore containing 7.25 ppm Au. R-mode factor analysis of data for 37 elements collected along four profiles across the sample yielded the following trace element association in ore stage pyrite: As, Tl, Hg, Sb, Au, Cs, Cu, in decreasing magnitude of factor score. Ag is not present in this factor and Au/Ag ratios in ore-stage pyrite typically range between 10 and 30. Ore-stage pyrite contains between 2 and 5 wt percent As and 50 to 500 ppm Au. Whereas the element association and measured As concentrations are similar to those of ore-stage pyrite in large Carlin-type deposits in other districts (e.g. Emsbo et al., 2003), the Au concentrations are an order of magnitude lower. Assuming that precipitation mechanisms were similar in each of these districts, the results suggest that ore fluids in the Alligator Ridge district had lower Au concentrations. This conclusion is consistent with the lower solubility of Au in the Alligator Ridge low-temperature fluids and helps explain the low grade and small size of the gold deposits.

Acknowledgments

We thank Placer Dome North America, Inc., for access to information and discussions with numerous geologists including Bill Howald and Bill Stout. At the U.S. Geological Survey, we also wish to thank Poul Emsbo, William D. Christiansen, F.G. (Barney) Poole, and Anita G. Harris for electron microprobe and stable isotope analyses, information, and helpful discussions. John Muntean and Alan Wallace provided constructive reviews of an earlier version of the manuscript.

REFERENCES

Arehart, G.B., Kesler, S.E, O'Neil, J.R., and Foland, K.A., 1992, Evidence for the supergene origin of alunite in sediment-hosted micron gold deposits, Nevada: ECONOMIC GEOLOGY, v. 87, p. 263–270.

Armstrong, R.L., 1968, Sevier orogenic belt in Nevada and Utah: Geological Society of America Bulletin, v. 79, p. 429–458.

Bodnar, R.J., Reynolds, T.J., and Kuehn, C.A., 1985, Fluid inclusion systematics in epithermal systems: Reviews in Economic Geology, v. 2, p. 74–98.

Brooks, W.E., Thorman, C.H., and Snee, L.W., 1995, The $^{40}Ar/^{39}Ar$ ages and tectonic setting of the middle Eocene northeast Nevada volcanic field: Journal of Geophysical Research, B, Solid Earth and Planets, v. 100, no. 6, p. 10,403–10,416.

Cecile, M.P., Shakur, M.A., and Krouse, H.R., 1983, The isotopic composition of western Canadian barites and the possible derivation of oceanic sulphate $\delta^{34}S$ and $\delta^{18}O$ age curves: Canadian Journal of Earth Science, v. 20, p. 1528–1535.
Chacko, T., Mayeda, T.K., Clayton, R.N., and Goldsmith, J.R., 1991, Oxygen and carbon isotope fractionations between CO_2 and calcite: Geochimica et Cosmochimica Acta, v. 55, p. 2867–2882.
Christiansen, R.L, Yeats, R.S., Graham, S.A., Niem, W.A., Niem, A.R., and Snavely, P.D., Jr., 1992, Post-Laramide geology of the U.S. cordilleran region: Geological Society of America, Geology of North America, v. G–3, p. 261–406.
Clark, T.M., and Ehman, K.D., 1985, Late Eocene extensional faulting in the northern Basin and Range province, Elko County, Nevada [abs.]: Geological Society of America Abstracts with Programs, v. 17, no. 6, p. 348.
Clayton, R.N., and Mayeda, T.K., 1963, The use of bromine pentafluoride in the extraction of oxygen from oxides and silicates for isotopic analysis: Geochimica et Cosmochimica Acta, v. 27, p. 43–52.
Dickinson, W.R., 2001, Tectonic setting of the Great basin through geologic time: Implications for metallogeny: Geological Society of Nevada Special Publication 33, p. 27–53.
——2002, The Basin and Range province as a composite extensional domain: International Geology Review, v. 44, p. 1–38.
Dong, G., Morrison, G., and Jaireth, S., 1995, Quartz textures in epithermal veins, Queensland—classification, origin, and implication: ECONOMIC GEOLOGY, v. 90, p. 1841–1856.
Emsbo, P., Hofstra, A.H., Park, D., Zimmerman, J.M., and Snee, L., 1996, A mid-Tertiary age constraint on alteration and mineralization in igneous dikes on the Goldstrike property, Carlin trend, Nevada [abs.]: Geological Society of America Abstracts with Programs, v. 28, no. 7, p. 476.
Emsbo, P., Hutchinson, R.W., Hofstra, A.H., Volk, J.A., Bettles, K.H., Baschuk, G.J., and Johnson, C.A., 1999, Syngenetic Au on the Carlin trend: Implications for Carlin-type deposits: Geology, v. 27, p. 59–62.
Emsbo, P., Hofstra, A.H., Lauha, E.A., Griffin, G.L., and Hutchinson, R.W., 2003, Origin of high-grade gold ore and source of ore fluid components in the Meikle gold deposit, northern Carlin trend, Nevada: ECONOMIC GEOLOGY, v. 98, p. 1069–1105.
Fouch, T.D., Hanley, J.H., and Forester, R.M., 1979, Preliminary correlation of Cretaceous and Paleogene lacustrine and related nonmarine sedimentary and volcanic rocks in parts of the eastern Great Basin of Nevada and Utah: Rocky Mountain Association of Geologists-Utah Geological Association, Basin and Range Symposium and Great Basin Field Conference, Las Vegas, Nevada, Oct. 7–11, 1979, p. 305–312.
Fouch, T.D., Potter, C.J, and Dubiel, R.F., 1992, Evolution of Maastrichtian and Paleogene lake basins and associated terranes, eastern Great Basin, Nevada [abs.]: Geological Society of America Abstracts with Programs, v. 24, no. 6, p. 12.
Fournier, R.O., 1985, The behavior of silica in hydrothermal solutions: Reviews in Economic Geology, v. 2, p. 45–62.
Gammons, C.H., and Williams-Jones, A.E., 1995, Hydrothermal geochemistry of electrum: Thermodynamic constraints: ECONOMIC GEOLOGY, v. 90, p. 420–432.
Gans, P.B., 2000, The northern White Pine Range, *in* Gans, P.B., and Seedorff, E., eds., Cenozoic tectono-magmatic evolution of White Pine County, Nevada: Core complexes, Eocene-Oligocene volcanic centers, episodic extension and shortening, and disseminated gold deposits: Geological Society of Nevada Symposium Geology and Ore Deposits 2000: The Great Basin and Beyond, Reno/Sparks, Nevada, May 15–18, 2000, Field Trip 11, p. 83–95.
Gans, P.B., Seedorff, E., Fahey, P.L., Hasler, R.W., Maher, D.J., Jeanne, R.A., and Shaver, S.A., 2001, Rapid Eocene extension in the Robinson district, White Pine County, Nevada: Constraints from $^{40}Ar/^{39}Ar$ dating: Geology, v. 29, p. 475–478.
Giesemann, A., Jager, H.J., Norman, A.L., Krouse, H.R., and Brand, W.A., 1994, On-line sulfur isotope determination using elemental analyzer coupled to a mass spectrometer: Analytical Chemistry, v. 66, no. 18, p. 2816–2819.
Good, S.C., 1987, Mollusc-based interpretations of lacustrine paleoenvironments of the Sheep Pass Formation (latest Cretaceous to Eocene) of east-central Nevada: Palaios, v. 2, p. 467–478.
Grauch, V.J.S., 1996, Magnetically interpreted granitoid plutonic bodies: Nevada Bureau of Mines and Geology Open-File Report 96–2, p. 7.1–7.16.
Haynes, S.R., Hickey, K.A., Mortensen, J.K., and Tosdal, R.M., 2002, Onset of extension in the Basin and Range: basin analysis of the Eocene Elko Formation, NE Nevada [abs.]: Geological Society of America Abstracts with Programs, v. 34, no. 6, p. 85.
Henry, C.D., and Boden, D.R., 1998, Eocene magmatism: The heat source for Carlin-type gold deposits of northern Nevada: Geology, v. 26, p. 1067–1070.
Hitchborn, A.D., Arbonies, D.G., Peters, S.G., Connors, K.A., Noble, D.C., Larson, L.T., Beebe, J.S., and McKee, E.H., 1996, Geology and gold deposits of the Bald Mountain mining district, White Pine County, Nevada, *in* Coyner, A.R., and Fahey, P.L., eds., Geology and ore deposits of the American cordillera: Reno, Geological Society of Nevada, Symposium proceedings, p. 505–546.
Hofstra, A.H., and Cline, J.S., 2000, Characteristics and models for Carlin-type gold deposits: Reviews in Economic Geology, v. 13, p. 163–220.
Hofstra, A.H., Leventhal, J.S., Northrop, H.R., Landis, G.P., Rye, R.O., Birak, D.J., and Dahl, A.R., 1991, Genesis of sediment-hosted disseminated gold deposits by fluid mixing and sulfidization: Chemical-reaction-path modeling of ore-depositional processes documented in the Jerritt Canyon district, Nevada: Geology, v. 19, p. 36–40.
Hofstra, A.H., Snee, L.W., Rye, R.O., Folger, H.W., Phinisey, J.D., Loranger, R.J., Dahl, A.R., Naeser, C.W., Stein, H.J., and Lewchuk, M., 1999, Age constraints on Jerritt Canyon and other Carlin-type gold deposits in the western United States: Relationship to mid-Tertiary extension and magmatism: ECONOMIC GEOLOGY, v. 94, p. 769–802.
Hose, R.K., and Blake, M.C., Jr., 1976, Geology and mineral resources of White Pine County, Nevada, Part I, Geology: Nevada Bureau of Mines and Geology Bulletin 85, p. 1–35.
Howald, W.C., 1996, A brief history and geologic overview of the Vantage deposits, Alligator Ridge, Nevada: Geological Society of Nevada Special Publication 23, p. 87–104.
Howard, K.A., 1992, Ruby Mountains metamorphic core complex: Deep crustal exposures exhumed from beneath the Pinon Range?, *in* Trexler, J.H., Flanigan, T.E., Flanigan, D.M.H., Hansen, M., and Garside, L., eds., Structural geology and petroleum potential of southwest Elko County, Nevada: Reno, Nevada Petroleum Society Annual Field Trip Guide Book, June 5–7, 1992, p. 57–60.
Hulen, J.B., and Collister, J.W., 1999, The oil-bearing, Carlin-type gold deposits of the Yankee basin, Alligator Ridge district, Nevada: ECONOMIC GEOLOGY, v. 94, p. 1029–1049.
Hulen, J.B., Pinnell, M.L., Nielson, D.L., Cox, J.W., and Blake, J., 1994, The Yankee mine oil occurrence, Alligator Ridge district, Nevada—an exhumed and oxidized, paleogeothermal oil reservoir, *in* Schalla, R.W., and Johnson, E.H., eds., Oil fields of the Great basin: Reno, Nevada Petroleum Society, p. 131–142.
Hunt, J.M., 1996, Petroleum geochemistry and geology, 2nd edition: New York, W.H. Freeman and Company, 743 p.
Ilchik, R.P., 1990a, Geology and geochemistry of the Vantage gold deposits, Alligator Ridge-Bald Mountain mining district, Nevada: ECONOMIC GEOLOGY, v. 85, p. 50–75.
——1990b, Geology and genesis of the Vantage gold deposits, Alligator Ridge-Bald Mountain mining district, Nevada: Unpublished Ph.D. thesis, Los Angeles, California, University of California at Los Angeles, 138 p.
Ilchik, R.P., and Barton, M.D., 1997, An amagmatic origin of Carlin-type gold deposits: ECONOMIC GEOLOGY, v. 92, p. 269–288.
Ilchik, R.P., Brimhall, G.H, and Schull, H.W., 1986, Hydrothermal maturation of indigenous organic matter at the Alligator Ridge gold deposits, Nevada: ECONOMIC GEOLOGY, v. 81, p. 113–130.
Ketner, K.B., and Alpha, A.G., 1992, Mesozoic and Tertiary rocks near Elko, Nevada—evidence for Jurassic to Eocene folding and low-angle faulting: U.S. Geological Survey Bulletin 1988–C, p. C1–C13.
Klessig, P.J., 1984, History and geology of the Alligator Ridge gold mine, White Pine County, Nevada: Arizona Geological Society Digest, v. 15, p. 77–88.
Lee, J., 1995, Rapid uplift and rotation of mylonitic rocks from beneath a detachment fault: Insights from potassium feldspar $^{40}Ar/^{39}Ar$ thermochronology, northern Snake Range, Nevada: Tectonics, v. 14, p. 54–77.
Maher, B.J., 1997, Mississippian sedimentary rock-hosted gold deposits of the eastern Great basin: Relative importance of stratigraphic and structural ore controls: Society of Economic Geologists Guidebook Series, v. 28, p. 171–182.
McGrew, A.J., and Snee, L.W., 1994, $^{40}Ar/^{39}Ar$ thermochronologic constraints on the tectonothermal evolution of the northern East Humboldt Range metamorphic core complex, Nevada: Tectonophysics, v. 238, p. 425–450.

McGrew, A.J., Peters, M.T., and Wright, J.E., 2000, Thermobarometric constraints on the tectonothermal evolution of the East Humboldt Range metamorphic core complex, Nevada: Geological Society of America Bulletin, v. 112, p. 45–60.

Miller, D.M., Hillhouse, W.C., Zartman, R.E., and Lanphere, M.A., 1987, Geochronology of intrusive and metamorphic rocks in the Pilot Range, Utah and Nevada, and comparison with regional patterns: Geological Society of America Bulletin, v. 99, p. 866–879.

Miller, E.L., Dumitru, T.A., Brown, R.W., and Gans, P.B., 1999, Rapid Miocene slip on the Snake Range-Deep Creek Range fault system, east-central Nevada: Geological Society of America Bulletin, v. 111, p. 886–905.

Mortensen, J.K., Thompson, J.F.H., and Tosdal, R.M., 2000, U-Pb age constraints on magmatism and mineralization in the northern Great Basin, Nevada, *in* Cluer, J.K., Price, J.G., Struhsacker, E.M., Hardyman, R.F., and Morris, C.L., eds., Geology and ore deposits 2000: The Great Basin and beyond. Reno, Geological Society of Nevada, Symposium proceedings, p. 419–438.

Murowchick, J.B., 1992, Marcasite inversion and petrographic determination of pyrite ancestry: ECONOMIC GEOLOGY, v. 87, p. 1141–1152.

Nutt, C.J., 2000, Geologic map of the Alligator Ridge area, including the Buck Mountain East and Mooney Basin Summit quadrangles and parts of the Sunshine Well NE and Long Valley Slough quadrangles, White Pine County, Nevada: U.S. Geological Survey Miscellaneous Field Investigations Map I–2691, scale 1:24,000.

Nutt, C.J., and Good, S.C., 1998, Recognition and significance of Eocene deformation in the Alligator Ridge area, central Nevada: U.S. Geological Survey Open-File Report 98–338, p. 141–150.

Nutt, C.J., Hofstra, A.H., Hart, K.S., and Mortensen, J.K., 2000, Structural setting and genesis of gold deposits in the Bald Mountain-Alligator Ridge area, east-central Nevada, *in* Cluer, J.K., Price, J.G., Struhsacker, E.M., Hardyman, R.F., and Morris, C.L., eds., Geology and ore deposits 2000: The Great Basin and beyond: Reno, Geological Society of Nevada, Symposium proceedings, p. 513–537.

Ohmoto, H., and Rye, R.O., 1979, Isotopes of sulfur and carbon, *in* Barnes, H.L., ed., Geochemistry of hydrothermal ore deposits, 2nd edition: New York, John Wiley and Sons, p. 509–567.

O'Neil, J.R., Clayton, R.N., and Mayeda, T.K., 1969, Oxygen isotope fractionation in divalent metal carbonates: Journal of Chemical Physics, v. 51, p. 5547–5558.

Papke, K.G., 1984, Barite in Nevada: Nevada Bureau of Mines and Geology Bulletin 98, 125 p.

Plumlee, G.S., and Rye, R.O., 1992, Mineralogic, isotopic, and other characteristics of the fringes of diverse hydrothermal systems: The perithermal environment [abs.]: V.M. Goldschmidt Conference, 3rd, Reston, Virginia, May 2-9, 1992, Proceedings, p. A84–A85.

Ponce, D.A., 1991, Gravity and magnetic anomalies in the Ely quadrangle, Nevada, and anomalies related to granitic plutons, *in* Raines, G.L., Lisle, R.E., Schafer, R.W., and Wilkinson, W.H., eds., Geology and ore deposits of the Great Basin. Reno, Geological Society of Nevada, Symposium proceedings, p. 103–106.

Potter, C.J., Dubiel, R.F., Snee, L.W., and Good, S.C., 1995, Eocene extension of early Eocene lacustrine strata in a complexly deformed Sevier-Laramide hinterland, northwest Utah and northeast Nevada: Geology, v. 23, p. 181–184.

Rahl, J.M., McGrew, A.J., and Foland, K.A., 2002, Transition from contraction to extension in the northeastern Basin and Range: New evidence from the Copper Mountains, Nevada: Journal of Geology, v. 110, p. 179–194.

Ressel, M.W., Noble, D.C., Henry, C.D., and Trudel, W.S., 2000, Dike-hosted ores of the Beast deposit and the importance of Eocene magmatism in gold mineralization of the Carlin trend, Nevada: ECONOMIC GEOLOGY, v. 95, p. 1417–1444.

Ridley, W.I., 2000, The ICP-MS laser microprobe: A new geochemical tool: Trends in Geochemistry, v. 1, p. 1–14.

Rigby, J.K., 1960, Geology of the Buck Mountain-Bald Mountain area, southern Ruby Mountains, White Pine County, Nevada: Intermountain Association of Petroleum Geologists and Eastern Nevada Geological Society Annual Field Conference, 11th, Salt Lake City, Utah, 1960, Guidebook, p. 173–180.

Rimstidt, J.D., 1997, Gangue mineral transport and deposition, *in* Barnes, H.L., ed., Geochemistry of hydrothermal ore deposits, 3rd edition: New York, John Wiley and Sons, p. 487–516.

Rodriguez, B.D., and Williams, J.M., 2001, Deep regional resistivity structure across the Battle Mountain-Eureka and Carlin trends, north-central Nevada: U.S. Geological Survey Open-File Report 01–346, 165 p.

Rye, R.O., Shawe, D.R., and Poole, F.G., 1978, Stable isotope studies of bedded barite at East Northumberland Canyon in the Toquima Range, central Nevada: U.S. Geological Survey Journal of Research, v. 6, p. 221–229.

Sheppard, S.M.F., and Gilg, H.A., 1996, Stable isotope geochemistry of clay minerals: Clay Minerals, v. 31, p. 1–24.

Simmons, S.F., and Browne, P.R.L., 2000, Hydrothermal minerals and precious metals in the Broadlands-Ohaaki geothermal system: Implications for understanding low-sulfidation epithermal environments: ECONOMIC GEOLOGY, v. 95, p. 971–999.

Solomon, B.J., McKee, E.H., and Andersen, D.W., 1979, Stratigraphy and depositional environments of Paleogene rocks near Elko, Nevada, *in* Armentrout, J.M., Cole, M.R., and TerBest, H., eds., Cenozoic paleogeography of the western United States: Anaheim, California, Society of Economic Paleontologists and Mineralogists, Pacific Section, p. 75–88.

Stock, J., and Molnar, P., 1988, Uncertainties and implications of the Late Cretaceous and Tertiary position of North America relative to the Farallon, Kula, and Pacific plates: Tectonics, v. 7, p. 1339–1384.

Stout, B., 1996, Geologic overview of the Yankee mine, White Pine County, Nevada: Geological Society of Nevada Special Publication 23, p. 105–110.

Tapper, C.J., 1986, Geology and genesis of the Alligator Ridge mine, White Pine County, Nevada: Nevada Bureau of Mines and Geology Report 40, p. 85–103.

Teal, L., and Wright, J., 2000, Geologic and geophysical overview of the Carlin trend, Nevada, *in* Cluer, J.K., Price, J.G., Struhsacker, E.M., Hardyman, R.F., and Morris, C.L., eds., Geology and ore deposits 2000: The Great basin and beyond. Symposium proceedings: Reno, Geological Society of Nevada, p. 567–570.

Vikre, P.G., 2000, Subjacent crustal sources of sulfur and lead in eastern Great basin metal deposits: Geological Society of America Bulletin, v. 112, p. 764–782.

Wells, M.L, Snee, L.W., and Blythe, A.E., 2000, Dating of major normal fault systems using thermochronology; an example from the Raft River detachment, Basin and Range, western United States: Journal of Geophysical Research, sec. B, v. 105, p. 16,303–16,327.

Wickham, S.M., Peters, M.T., Fricke, H.C., and O'Neil, J.R., 1993, Identification of magmatic and meteoric fluid sources and upward and downward-moving infiltration fronts in a metamorphic core complex: Geology, v. 21, p. 81–84.

Wilder, A.M., and Seward, T.M., 2002, The adsorption of gold(I) hydrosulfide complexes by iron sulphide surfaces: Geochimica et Cosmochimica Acta, v. 66, p. 383–402.

Wooden, J.L., Kistler, R.W., and Tosdal, R.M., 1998, Pb isotope mapping of crustal structure in the northern Great Basin and relationships to Au deposit trends: U.S. Geological Survey Open-File Report 98–338, p. 20–33.

Zheng, Y.-Z., 1993, Calculation of oxygen isotope fractionations in anhydrous silicate minerals: Geochimica et Cosmochimica Acta, v. 57, p. 1079–1091.